Methods for Representing Earthquake Time Series with Networks

Romi Koželj[1], Lovro Šubelj[1,2] and Jurij Bajc[3]
[1]University of Ljubljana, Faculty of Computer and Information Science, Ljubljana, Slovenia
[2]University of Ljubljana, Faculty of Social Sciences, Ljubljana, Slovenia
[3]University of Ljubljana, Faculty of Education, Ljubljana, Slovenia
E-mail: romi.kozelj@gmail.com, lovro.subelj@fri.uni-lj.si, jurij.bajc@pef.uni-lj.si

Keywords: network analysis, seismic activity, earthquakes, time series

Received: September 10, 2023

An earthquake is a natural phenomenon that occurs as a result of the internal dynamics of the Earth. It originates deep below the surface of the planet and cannot be predicted with our current knowledge. In this paper, we use a network analysis approach to analyze the characteristics and evolution of seismic activity over time. We implement several network models based on temporal and spatial interactions between earthquakes and on the assumption of self-similarity of seismic activity in selected geographic areas. We create sequences of networks generated in consecutive time windows and compare the networks between different models and time intervals. Additionally, we calculate a set of network structural characteristics and study their changes over time. The analysis shows that most models produce networks with such a structure that changes consistently with the intensity of seismic activity. Thus, based on the structural changes of networks, we can reliably identify the time windows with increased seismic activity.

Povzetek: V članku je predstavljena analiza značilnosti in razvoja seizmične aktivnosti skozi čas z uporabo analize omrežij.

1 Introduction

Earthquakes are typically caused by the release of stress that builds up on faults at the junctions of lithospheric plates. Block movement during an earthquake changes the stress field, affecting seismic activity development in the wider area [1]. The occurrence of earthquakes is influenced by various factors, such as the size of the fault and the amount of stress accumulated next to it. To directly measure the likelihood of earthquake occurrences in a specific area, one would need to measure the amount of stress accumulated several kilometers under the surface of the Earth, which is technologically challenging. Additionally, the values of other parameters that affect the amount of stress required to cause plate slippage vary from fault to fault [2]. Some procedures have been developed that can help determine the areas where an earthquake may occur and estimate the maximum expected magnitude with a certain probability [3, 4]. Nevertheless, modern science does not yet have the tools to determine the location, the magnitude, and the time of an earthquake with an accuracy that would have practical significance [2].

This study focuses on analyzing seismic activity over time from the network science perspective. We analyze and compare seismic activity patterns in consecutive time windows of data, where we use various methods of capturing and representing the data. The observations give interesting insights into the development of seismicity, considering the effect of earthquakes on each other. The proposed approach may offer a new way of processing seismic data that could potentially be used to reason about seismic behaviour in the near future.

Because it is difficult to consider all the factors that influence the occurrence of earthquakes [5], it is helpful to use new approaches that do not require an understanding of the entire dynamics of earthquake occurrence. The seismic data analyzed in this paper consist of the locations of the focuses, the times when the earthquakes occurred, and their magnitudes. Such data is usually represented in tabular form, where the hidden information about their interactions are ignored. The advantage of representing seismic data with a network is that it can capture the information about interactions and reveal hidden patterns in correlations between earthquakes.

In this study we use public seismic catalogs for Italy, Japan, Southern California and Northern California. The span of earthquakes in each catalog is divided evenly into several consecutive time intervals. For each time interval, we construct multiple networks, which are built using the existing methods [6, 7, 8, 9, 5, 10, 11] and also a new method created as a combination of the published ones. Analyzing one model at the time, networks constructed in time intervals with higher seismic activity are compared to those constructed in time intervals with lower seismic activity. Networks constructed in the same time intervals are also compared across different network models.

Finally, using generated sequences of networks, we calculate a set of network characteristics and assemble them

into time series. We study whether changes in time series can indicate in which time intervals seismic activity increases and if time series show any specific change in seismicity before a stronger earthquake occurs. The study is contrived to also enable the application of predictive models for time series analysis to test whether values in time series can be predicted.

The rest of the paper is organized as follows. Section 2 surveys related works. In section 3, we introduce the data and preprocessing techniques to obtain complete datasets. In section 4, we present the approach for generating sequences of networks. Firstly, section 4.1 proposes a method for dividing time ranges of catalogs into smaller intervals. In section 4.2, we explain the technique for constructing nodes of networks, and lastly, in section 4.3, we present the adopted network models. Section 5 compares the generated networks and section 6 analyzes time series from selected network characteristics. In section 7, we end the paper with conclusions and a discussion of future work.

2 Related works

In this section, we summarize the results of other studies that used network constructions analyzed in this paper, omitting the explanation of these networks as they are explained in section 4.3. For clarity, studies are further summarised in Table 1.

Abe Sumiyoshi et al. [6] generated networks according to the NTS(C) construction (section 4.3.1), where each network was built using a large portion of the catalog. They analyzed the dependence of the clustering coefficient C and the exponent γ of the power-law distribution on the size of the cell. Results show that both parameters stop changing when the cell size exceeds a certain threshold value. They also observed that generated NTSC(C) networks are scale-free and small-word.

Abe Sumiyoshi et al. [14] constructed NTS(C) networks in successive time intervals around times of larger earthquakes and observed the evolution of the clustering coefficient of these networks. They show that around the time of a large event, the clustering coefficient displays a characteristic behavior; it suddenly jumps at the time of a large earthquake and then slowly decays until it becomes stationary again following the power law distribution.

Telesca Luciano et al. [9] generated VG(E) networks (section 4.3.4) and analyzed the derived degree distributions. Networks were constructed using only earthquakes above a chosen threshold magnitude value, increasing this value from 1.9 to 3.5 with the step of 0.1. Acquired degree distributions do not change significantly for different threshold magnitude values and are power law shaped, indicating a scale-free nature of these networks.

They also investigated the dependency of the VG(E) structure with respect to time and considered series of earthquakes occurring regularly and those with randomly shuffled inter-event times. Study shows that there is no significant difference between the degree distributions of the original earthquake sequence and the shuffled sequences. They argue that VG(E) structure depends only on the values of the magnitude.

Soghra Rezaei et al. [5] generated NTS(C) and VG(C/E) (section 4.3.4) networks. For each NTS(C) network they also considered only the events above some threshold magnitude value, increasing this value for each generated network. They observed that the number of links in these networks has a Gutenberg-Richter law relationship with the threshold magnitude value. Gutenberg-Richter law was also obtained for the VG(C) network, where the power law relationship with the threshold magnitude value was observed for the number of nodes in the network.

For VG(E) and VG(C) networks, they analyzed the frequency with which new links connected to some larger earthquake are added to the network when the network grows over time with new occurring earthquakes. Study indicates that this frequency, with respect to time, mimics the Omori law.

Joel N. Tenenbaum et al. [10] constructed networks according to the NCV(C) construction (section 4.3.6), where they analyzed the strength of the obtained connections. The time interval in which networks were built was divided into 90-day long non-overlapping subintervals representing the cell vectors. Vector values were constructed by calculating the sum of earthquake magnitudes (SM), the average magnitude (AM), the number of events (NE), and the energy released by earthquakes (ER) in each of the subintervals. The analysis shows large correlations between cells more than 1000 km apart in these networks. They also split the catalog into two parts along the time axis of the catalog and constructed partly overlapping networks. Study shows that the obtained networks consist of significant structural similarities.

Nastaran Lofti et al. [11] divided the time span of earthquakes in a catalog in multiple overlapping intervals in which they constructed the MLN-NTS(C) networks (section 4.3.7). They calculated the eigenvector centrality (a network property) and the total magnitude of earthquakes (an earthquake property) from each of the networks and analyzed the correlation between these properties. Analysis was done on networks with one, two, three, and four layers. Results show a higher correlation in networks with three or four layers versus one-layer networks, which indicates that multilayer structure better captures earthquake dynamics over time.

They also verified that adjacent cells present similar activity patterns by projecting cells into two-dimensional space. This was done using the Principal Component Analysis (PCA) which removed the correlation between the node centrality in different layers.

Xuan He et al. [7] constructed NTSW(C) networks (section 4.3.2). They show that the degree distribution of these networks obeys power law, consequently making networks scale-free. Since the frequency of earthquakes with large magnitudes also decays as a power law, the scale-

Table 1: Summary of related works. The notation C_d denotes the cell size (cell edge length) in a network, N_t denotes the number of time intervals, $|t|$ denotes the length of the time intervals, and $|t_{lag}|$ denotes the length of the time lag between the time intervals for a series of networks. The abbreviation G-R stands for the Gutenberg-Richter law. Only the sources of the catalogs that are used in this paper are cited.

ref.	region	network		sequence			findings
		model	C_d [km]	N_t	$\|t\|$	$\|t_{lag}\|$	
[6]	S. California [12]	NTS(C)	various sizes (3D)	1	23 years	0	• scale-free and small-world • C and γ take the universal invariant values 0.85 and 1, respectively, when cell size becomes larger than a certain threshold
	Japan [13]				5 years		
	Iran				3 years		
	Chile				7 years		
[14]	S. California [12]	NTS(C)	5, 10 (3D)	$\approx$ 40 to 70	240 days, 24 days	0	• C remains stationary before the large earthquake, suddenly jumps at the event, then slowly decays to stationarity again
[9]	Italy [15]	VG(E)	/	1	5.7 years	0	• scale-free • similar degree distributions for different threshold magnitudes • VG(E) structure depends only on the magnitude values
[5]	Iran, California, Italy-Greece	NTS(C), VG(E), VG(C)	$\approx$ 4 to 220 (2D)	$\approx$ 10 to 20 for the Omori law, otherwise 1	7 years for the G-R law, otherwise less but grows	network grows over time for the Omori law with the lag $\approx$ 100 to 1000 hrs	• G-R law obtained for the NTS(C) and VG(C) networks • Omori law obtained for the VG(C/E) networks
[10]	Japan [16]	$\text{NCV(C)}^{SM}_{T=54}$, $\text{NCV(C)}^{ER}_{T=54}$, $\text{NCV(C)}^{NE}_{T=54}$, $\text{NCV(C)}^{AM}_{T=54}$	100 (2D)	1	entire catalog (13.5 years)	0	• strong links found representing large correlations between patterns located more than 1000 km apart • ~~networks of different periods~~ are structurally similar
		$\text{NCV(C)}_{T=28}$		2	7 years	not stated	
[11]	N. California [17]	MLN-NTS(C)$_{T=1}$, MLN-NTS(C)$_{T=2}$, MLN-NTS(C)$_{T=3}$, MLN-NTS(C)$_{T=4}$	75 (2D)	8	3 years	1 year	• earthquake dynamic is better captured with a multilayer structure • nearby regions have similar seismic activity patters
	Iran		66×55 (2D)				
[7]	S. California [12]	NTSW(C)	5, 10, 15, 20 (2D)	10 for the small-world concept, otherwise 1	1 year (small-world), 10 years, 20 years	0	• scale-free and small-world • G-R law obtained • Omori law obtained
[8]	S. California [12]	NHTSW(E)	/	1	17 years	0	• aftershocks identification • Omori law obtained • power law distribution of link weights and distances found

free nature of the degree distribution is consistent with the Gutenberg-Richter law.

They calculated the clustering coefficient and the average shortest path for networks constructed in consecutive one year time intervals. The clustering coefficient showed to be much larger than in random networks, while the average shortest path was very small. Both results indicate a small-world structure of NTSW(C) networks. Furthermore, the Omori law emerged as a result of counting the out-degree links of nodes containing large earthquakes over time in one year networks.

Marco Baiesi et al. [8] generated NHTSW(C) networks (section 4.3.3), where they dealt with the subject of aftershocks identification. Each earthquake in this network is connected to those earthquakes back in time that have triggered the event with a high probability. The links in the network were determined by selecting the largest (threshold) value $(n_{ij})_{max}$, before which the fully connected network breaks into clusters. The threshold value was obtained from the graph showing the size distribution of the connected components depending on the selected values of n_{ij}. They determined the point at which the smaller components merge into one larger one and set the value of n_{ij} at this point as $(n_{ij})_{max}$.

The Omori law was obtained for this network, as the number of outgoing links was found to be scale-free. The distribution of link weights and the distribution of distances between earthquakes and their aftershocks exhibits a power law behaviour. They state that the fat tail of the distance distribution suggests that aftershocks collection with fixed space windows is not appropriate.

It can be observed that studies relevant to this paper focus primarily on investigating one network or, at most, a few networks from the entire catalog. However, the main feature of this study is examining the time evolution of networks and their characteristics where we consider a significant number of time points.

3 Data

We analyze the data of detected seismic activity in Japan, Italy, and California. The data was obtained from four online sources (Table 2).

Table 2: Seismic catalogs and online sources.

region	source
Japan	High Sensitivity Seismograph Network Laboratory [13]
Italy	National Institute of Geophysics and Volcanology [15]
N. California	Northern California Earthquake Data Center [17]
S. California	Southern California Earthquake Data Center [12]

Since the time span of California catalogs goes far back in time (from 1932 for Southern California and from 1966 for Northern California), we examine the number of earthquakes in individual years. Due to updates in seismological equipment and increase in the density of the network of seismic stations, the number of detected earthquakes increases from year to year up to 1981, when the seismic stations throughout California improved. We consider the data recorded after 1981 as more reliable and suitable for further analysis, and therefore limit these two catalogs only to the data from 1981 onwards.

Since both California catalogs cover the same geographical area, despite one containing earthquakes detected at stations in Northern California and the other at stations in Southern California, we also examine how much the number of earthquakes changes if the areas are reduced more to the north or to the south. We conclude that the earthquakes that occurred in Northern California were not well detected by the stations in Southern California, and vice versa. In the following, we therefore limit the area of Northern California to $35° \leq$ latitude $\leq 42°$ and $-125° \leq$ longitude $\leq -116°$, and the area of Southern California to $32° \leq$ latitude $\leq 37°$ and $-122° \leq$ longitude $\leq -114°$. If the areas are reduced further, the number of earthquakes decreases considerably, omitting relevant data.

One of the fundamental empirical laws in seismology is the Gutenberg-Richter law [18], which states that the number of earthquakes decreases exponentially with increasing magnitude. This is described by the relationship

$$\log_{10} N = a + bM, \tag{1}$$

where N denotes the number of earthquakes of magnitude M, and a and $b < 0$ are the corresponding constants. Figure 1 shows the number of detected earthquakes of a particular magnitude for Japanese and Italian catalogs.

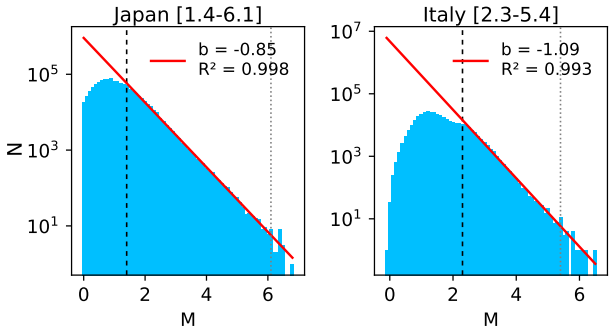

Figure 1: The number of detected earthquakes N of different magnitudes M for Japanese (left) and Italian (right) catalogs. The two vertical lines indicate the minimum and maximum magnitude thresholds that are also listed in square brackets at the top of the Figure.

One can observe that the linear relationship (1) does not apply to very weak earthquakes. Even though weaker earthquakes occur more frequently than stronger ones, they are often not detected by seismic observatories, since ground

shaking during weak earthquakes is only measurable close to the hypocenters. Thus, catalogs containing such earthquakes are incomplete. In order to obtain more complete catalogs, we determine a minimum magnitude threshold for each of the catalogs and keep only earthquakes with magnitudes above the threshold. Although this significantly reduces the amount of data, we know with a considerable degree of reliability that all earthquakes above the threshold are included in the data. The minimum magnitude thresholds are determined by maximizing the goodness of fit R^2 of the regression lines (1), while still trying to keep as much data as possible.

Since strong earthquakes are very rare, deviations from the linear dependence (1) occur also at high magnitudes. For this reason, we also define the maximum magnitude threshold for each catalog and omit all earthquakes above this threshold when determining the regression lines. We employ the fact that earthquakes occur according to the Poisson distribution $\frac{\lambda^k e^\lambda}{k!}$ [19, 20], which indicates the probability of the occurrence of k events in a certain time interval if the expected number of events in an interval equals to λ. The confidence interval for the Poisson distribution is $\lambda \pm \sigma$ with the standard deviation of $\sigma = \sqrt{\lambda}$. We determine a maximum magnitude threshold for each of the catalogs such that $\sigma/\lambda = 1/\sqrt{\lambda} \leq 0.5$.

Table 3 shows the number of earthquakes in catalogs before and after preprocessing, the minimum magnitude thresholds and the catalogs' time ranges.

Table 3: The size of the catalogs N before and after preprocessing of the data, the minimum magnitude thresholds M_{min} and the time ranges of complete catalogs.

region	N (before)	M_{min}	N (after)	time [years]
Japan	1 109 140	1.4	316 558	12
Italy	370 564	2.3	61 708	35
N. California	967 897	1.6	213 061	39
S. California	751 491	1.6	233 250	39

4 Methodology

In this section, we describe the generation of sequences of networks. This includes explanation of division of catalogs' time ranges into smaller consecutive time intervals, description of the technique used to cut the Earth's interior into smaller pieces to obtain nodes of generated networks, and presentation of network models.

4.1 Time intervals

The earthquake catalogs contain a different number of earthquakes that occurred in different time ranges (Table 2). When determining the length of time intervals in which we generate individual networks, we try to ensure the best possible comparability between networks across all earthquake catalogs. In addition, we want to create enough time intervals so that the time series containing the feature values calculated from the generated networks will contain enough points for a successful learning of the time series predictive model.

We decide that the time series should contain at least 200 points. One way to ensure the comparability of the generated networks is to predetermine the average number of earthquakes within individual time intervals $\langle e_t \rangle$ and keep this number the same for all earthquake catalogs. In this way, all generated networks on average consist of the same number of earthquakes.

Because a strong earthquake triggers many aftershocks, time intervals in which a stronger earthquake occurs contain a significantly higher number of events (Figure 2). Generating networks from a large number of events can result in slow execution of network model algorithms and slow calculation of network characteristics. Conversely, if the number of events is too small, the generated networks could be meaningless or incomparable since they would contain too little data.

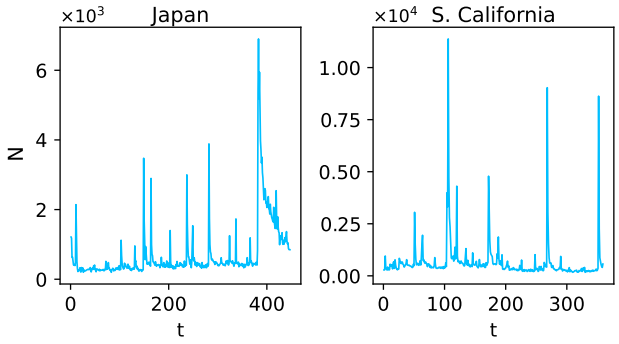

Figure 2: The number of earthquakes in each of the time intervals in the Japanese (left) and the S. California catalog (right). The time intervals are generated according to the data in Table 4.

Therefore, the search for the appropriate value $\langle e_t \rangle$ is started from larger values to smaller ones. We stop at values $600 \lesssim \langle e_t \rangle \lesssim 800$, which we accept as reasonable given the execution time of the algorithms within time intervals containing a large number of events. If the number of intervals calculated using such average number of earthquakes per interval is insufficient, the intervals are offset so that they partially overlap. This method increases the number of time intervals while maintaining the same average number of earthquakes per interval. The obtained time intervals are shown in Table 4.

Table 4: The number of time intervals N_t, the length of time intervals $|t|$, the length of the lag between the time intervals $|t_{lag}|$, and the average number of earthquakes $\langle e_t \rangle$ within time intervals. The average number of earthquakes is rounded to a whole number.

region	N_t	$\|t\|$ [days]	$\|t_{lag}\|$ [days]	$\langle e_t \rangle$
Japan	447	10	0	707
Italy	256	150	100	718
N. California	359	40	0	589
S. California	359	40	0	649

4.2 Division of Earth into cells

The nodes of most of the generated networks represent smaller, non-overlapping parts of the Earth's interior. We obtain them by cutting the area defined by the earthquake hypocenters of each catalog into 3D or 2D cells of approximately the same size. 3D cells are roughly cubes with approximately equally long edges in all three directions. They are generated by cutting the Earth along parallels, meridians, and in depth. 2D cells have a shape of upright prisms with a base face of a roughly square shape. They are generated by cutting the area only along the Earth's surface, i.e., along parallels and meridians, where each obtained part is stretched inward to the maximum depth of the area.

Because connections in networks are formed according to the interactions between the earthquakes located in the cells, we want the volumes of the cells to be as comparable as possible. Otherwise, larger cells could contain more earthquakes simply because of their size, thus forming more active nodes and a greater number of connections than smaller cells. The area is therefore cut so that the cells closer to the poles cover a larger angle of longitude than those closer to the equator, and the cells deeper in the Earth cover a larger angle of longitude and latitude than those closer to the surface (Figure 3). Table 5 shows the number

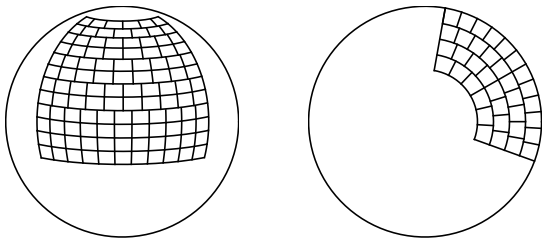

Figure 3: An example of generated cells from the areal view (right) and the vertical cross-section view (left).

of cells obtained when cutting geographic areas into 3D and 2D cells with edge lengths of about 5 km and 20 km.

When generating networks, we use 3D cells of sizes 5, 10, and 20 km and 2D cells of sizes 5 and 10 km. The chosen cell sizes are comparable to those used in the literature. It is important to note that if the cells used are too small, only the hypocenters, which are point size, are considered, while the earthquakes are much larger. On the other hand, using too large cells can cause a deterioration of spatial resolution.

Table 5: The number of cells containing at least one earthquake when cutting the areas into 3D and 2D cells with edge lengths of roughly 5 km and 20 km.

region	5 km (3D)	5 km (2D)	20 km (3D)	20 km (2D)
Japan	31 647	14 827	2 920	1 821
Italy	22 261	12 131	3 812	2 182
N. California	22 083	9 616	1 924	1 159
S. California	13 731	6 211	1 012	691

4.3 Network models

In this chapter, we describe network models used for constructing seismological networks. The nodes of some networks are represented by earthquakes that connect to each other based on their interactions. In other networks, nodes are represented by cells of a geographic area that are connected based on interactions between earthquakes located in the cells. For clarity, we label networks consisting of earthquakes with a mark (E) at the end of the network name and networks consisting of cells with a mark (C). All networks are analyzed as simple undirected unweighted networks.

4.3.1 Time sequence of earthquakes

The construction of the network based on time sequence of earthquakes NTS(C) [6] is built on the assumption that the spatial connectivity of seismic events is long-range since earthquakes can also appear as the cause of preceding very distant earthquakes [21, 22]. The nodes of this network are presented by cells of the geographic area. The connections between cells are generated by earthquakes that occur in time directly one after the other, regardless of their distance to each other. When implementing this network, we first arrange the earthquakes according to the time of their occurrence. Then, for each successive pair of earthquakes, we generate a connection between the corresponding cells[1].

4.3.2 Time-space windows

The construction of the network based on the time-space windows NTSW(C/E) [7] is created on the assumption that the elastic energy released during an earthquake causes the resulting seismic activity in the surrounding areas for a time interval t from the time of the earthquake. The area subjected to the influence of seismic waves is defined as a sphere with the center at the earthquake's focus and the radius R. Earthquakes with higher magnitudes affect the

[1] The nodes of NTS network cannot be presented by earthquakes since forming such connections between earthquakes would result in a "chain" network.

seismic activity of a wider area and for a longer time than earthquakes with lower magnitudes. The radius R of the surrounding area affected by an earthquake of magnitude M and the length of the time interval t are calculated according to equations

$$\log_{10} R = a_R M + b_R, \tag{2}$$

$$\log_{10} t = a_t M + b_t, \tag{3}$$

where a_R, b_R, a_t and b_t denote the corresponding constants [7].

Using equations (2) and (3), we generate a time-space window around the focal point of each earthquake in the catalog. The size of the window depends on the magnitude of the earthquake. An earthquake that generates a window triggers a link to each earthquake within that window. To calculate the distance between two earthquake focuses, we use the Euclidean distance. The values of parameters a_R, b_R, a_t and b_t for the area of S. California are determined in [23] by analyzing the seismic catalog and developing a new method for identifying the time $t(M)$ and space $R(M)$ intervals that include most of the aftershocks related to an earthquake of magnitude M.

Figure 4 shows earthquakes' spatial and temporal influence depending on the magnitude in the area of S. California with the associated parameters resulting from works [23, 7].

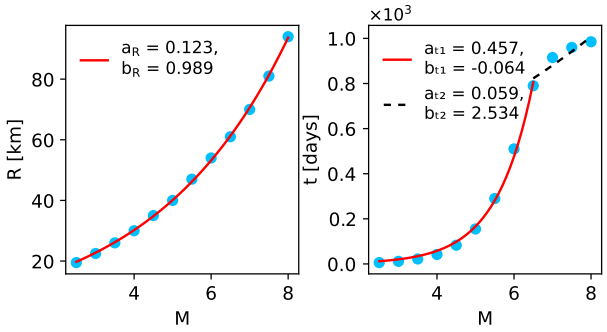

Figure 4: Spatial (left) and temporal (right) influence of earthquakes as a function of magnitude in the area of S. California. Adapted from [23, 7].

The dependencies show, for example, that an earthquake with a magnitude of $M = 6.5$ affects an area up to $R = 61$ km from the focus of the earthquake for a period of $t = 790$ days from the time of the earthquake. Since the curve presenting the time influence as a function of the magnitude breaks at the magnitude value $M = 6.5$, the time dependence is described by two pairs of parameters. In [7] it is stated that the different dependences of $t(M)$ at $M > 6.5$ and $M \leq 6.5$ are determined empirically. Arguments for the dual nature of this dependence are not provided.

The obtained parameter values depend on the observed geographic area [7]. The relevance of these parameters for Japan, Italy, or even N. California is, therefore, questionable. Since we do not have the data on aftershocks or the sizes of time-space windows for the rest of the Earth, and due to difficulty of obtaining these parameters, this network construction and the obtained parameters are only used on the S. California catalog. The nodes of this network can be presented by earthquakes (NTSW(E)) or by cells of the geographic area (NTSW(C)).

4.3.3 Hyperbolic time-space windows

The construction of the network based on hyperbolic time-space windows NHTSW(C/E) [8] is designed on a similar metric as the NTSW(C/E) construction, but instead of rectangular windows, the hyperbolic windows are introduced. The metrics used to define the hyperbolic windows takes into account that the impact of earthquakes decreases with time and distance (Figure 5).

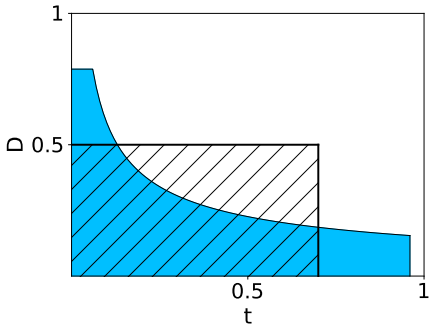

Figure 5: Schematic representation of the rectangular space-time window used in NTSW(C/E) (dashed rectangle) and the hyperbolic window used in NHTSW(C/E) (solid area). Units are arbitrary. Adapted from [8].

To determine the connections between earthquakes in a network, we need to calculate the expected number of earthquakes

$$n_{ij} = HtD^{fd}10^{-bM_i} \tag{4}$$

within the time-space window defined by each pair of earthquakes i and j. In equation (4), t represents the time difference between the occurrence of the two earthquakes ($t_i < t_j$), D is the distance between earthquakes' focuses, fd is the fractal dimension [24] of the geographic area where the two earthquakes occurred, and H is the corresponding constant. Variable M_i is the magnitude of the earthquake i and is represented via the Gutenberg Richter's law $N \propto 10^{bM_i}$ (equation (1)), $b < 0$).

Equation (4) shows that a shorter time t and a shorter distance D between two earthquakes both reduce the value of n_{ij}. The correlation value between earthquakes i and j is, consequently, inversely proportional to the value of n_{ij}. Using equation (4), we calculate the correlation value for each pair of earthquakes. Since the parameters t and D in equation (4) appear in the product, earthquake i can also be strongly correlated with earthquake j, which occurred at a greater distance in time and a smaller distance in space, or vice versa. Therefore, the resulting window is hyperbolic (Figure 5).

Fractal dimension fd is calculated using the box-counting method [8], where grids of different sizes are placed on the geographic area. For each grid size, we count the number of grid cells that contain at least one earthquake. In our case, the grid is represented by an arrangement of non-empty 3D cells. The fd value is calculated as the slope of the line representing $log(N)$ values as a function of the $log(Cd^{-1})$ values, where N is the number of non-empty grid cells, and Cd is the length of cell edges (Figure 6). We calculate the fd value for each of the catalogs.

From Figure 6 one can see that the number of non-empty cells in denser grids (the right part of graphs) changes differently as in the case of sparser grids (the left part of graphs). Because the relationship between the variables N and Cd^{-1} on a log-log scale must be linear, we use only the points corresponding to the linear relationship between the variables when determining the slope of the regression lines (Figure 6).

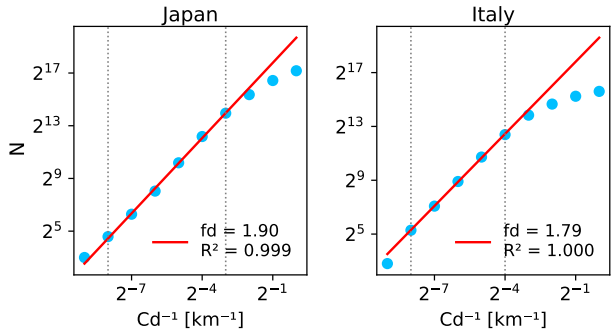

Figure 6: The number of non-empty cells N along the inverse value of the length of cell edges Cd^{-1} for the Japanese (left) and the Italian (right) catalog when the area is cut into 3D cells. The vertical dashed lines indicate the part of the data used to calculate the regression line.

Since we want to avoid generating networks that are to densely connected, we keep only a share of the most correlated connections. The number of connections is calculated by determining the average degree $\langle k \rangle$ in each network and keeping $\langle k \rangle$ the same for all constructed networks. This is a simple but valid way to ensure the comparability of the obtained networks. We use the relationship $\langle k \rangle = \frac{2m}{n}$ and calculate m at a value of $\langle k \rangle = 10$ [25], thus keeping $m = 5n$ of the most correlated links in the networks.

The nodes of this network can be earthquakes (NHTSW(E)) or cells of the geographic area (NHTSW(C)).

4.3.4 Visibility graph

In the construction of the visibility graph VG(C/E) [9, 5], the earthquakes represent the points of the graph that shows the time of the earthquakes on the x-axis and the magnitude of the earthquakes on the y-axis. Two earthquakes are connected if no other earthquake happened in the time between two earthquakes with a magnitude above the straight line connecting the points representing the initial two earthquakes. If such an earthquake would exist, it would "overshadow" the influence of the first earthquake on the second one; thus, the earthquakes would not "see" each other.

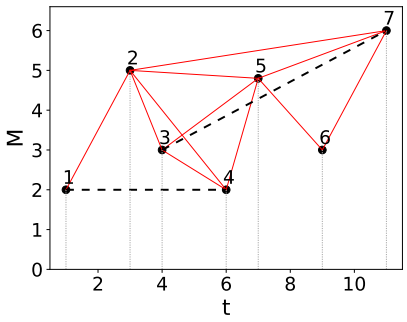

Figure 7: An example of a network corresponding to the visibility graph (links of a network are shown with solid lines) and an example of a network that does not correspond to the visibility graph (links of a network are shown with solid and dashed lines). Dots represent nodes of the network. Units are arbitrary.

Solid lines in Figure 7 show the links corresponding to the visibility graph since no point lies above any of the links. To make distinguishing between correct and incorrect connections in the network easier, we also show dotted vertical lines connecting the points with the x-axis. Solid lines show all possible connections between these points since no link can be made between any other pair of points.

Dashed lines in Figure 7 show two additional links added to the network that are inadequate since the link between earthquakes 1 and 4 is overshadowed by earthquakes 2 and 3, and the link between earthquakes 3 and 7 is overshadowed by earthquake 5. Therefore, the network containing these two links does not correspond to the construction of the visibility graph.

The nodes of the visibility graph can be earthquakes (VG(E)) or cells of the geographic area where instead of earthquakes we connect their corresponding cells (VG(C)).

4.3.5 Spatially upgraded visibility graph

Connections in the visibility graph are created without taking into account distances between earthquakes. Two earthquakes are connected if they "see" each other, even if they are very far apart.

We upgrade the visibility graph by generating a spatial window defined by equation (2) around the focal point of each earthquake. The size of the window depends on the magnitude of the earthquake. The parameters for generating the window are listed in the left part of Figure 4. Each earthquake is connected with all those earthquakes that are "visible" with the given earthquake and are also located within the corresponding spatial window. Consequently, the "visibility" between earthquakes is limited by their distance from each other. Earthquakes located outside of the

window cannot prevent connections in the window. We name this construction a spatially upgraded visibility graph SVG(C/E).

Nodes can be earthquakes (SVG(E)) or cells of the geographic area (SVG(C)). Due to the difficulty of obtaining the appropriate parameters in equation (2), the described network construction is only used on the S. California catalog (as the construction described in section 4.3.3).

4.3.6 Correlation between cell characteristics

In the construction of the network based on a correlation between vectors that represent cell characteristics NCV(C) [10], we assign a vector to each of the cells of the geographic area that contains at least one earthquake. The vector elements represent a chosen cell characteristic s in shorter consecutive time intervals. Cell vectors are constructed as follows. Firstly, we divide the time interval in which the network is generated into T equally long non-overlapping subintervals. Then, for each of the cells, we calculate a value for s using the earthquakes located in the cell within each subinterval. Those values represent vector elements.

Cells are connected based on the Pearson correlation coefficient r [26] between the corresponding vectors, where the correlation value represents the strength of the connection between two vectors. The value for r between vectors $\boldsymbol{x}$ and $\boldsymbol{y}$ is calculated using the equation

$$r = \frac{\sum_j (\boldsymbol{x}_j - \langle \boldsymbol{x} \rangle)(\boldsymbol{y}_j - \langle \boldsymbol{y} \rangle)}{\sqrt{\sum_j (\boldsymbol{x}_j - \langle \boldsymbol{x} \rangle)^2} \sqrt{\sum_j (\boldsymbol{y}_j - \langle \boldsymbol{y} \rangle)^2}} \tag{5}$$

with values expanding in the range [-1,1].

Because a strong correlation is represented in negative and positive correlation values, the most correlated links are those with a high absolute value of r. To avoid constructing too dense networks, we keep only those connections with $|r|$ greater than some predetermined threshold value r_{min}. The value for r_{min} is determined by analyzing the number of pairs of cells within interval $0.5 < |r| \leq 1$. In each of the catalogs, the number of cell pairs with $r = 1$ is much higher than the number of pairs with $0.5 < |r| < 1$. Additionally, the number of pairs with r values in $0.5 < |r| < 1$ are very low. Thus, choosing any r value in interval $0.5 < |r| < 1$ represents an equally good choice for r_{min} since the generated networks would contain approximately the same number of connections. We set r_{min} to 0.95.

We use two characteristics of cells – the sum of earthquake magnitudes ($\sum_i M_i$) and the amount of energy released by earthquakes ($\sum_i 10^{1.5M_i+16.1}$). We set the length of vectors to $T = 10$. In one case, we insert the sum of magnitudes as a characteristic into the cell vectors, and in the other, we insert the energy released by earthquakes. Then we increase T to 20 and repeat the process, getting four types of NCV(C) networks in total.

4.3.7 Multilayer network

The multilayer network MLN-NTS(C) [11] consists of several NTS(C) networks constructed in shorter consecutive time intervals. The time window in which the multilayer network is generated is again divided into T equally long non-overlapping subintervals. These subintervals represent layers of a mutlilayer network. Within each subinterval, we build a NTS(C) network. By connecting identical network cells in successive time intervals, we generate the MLN-NTS(C) network (Figure 8).

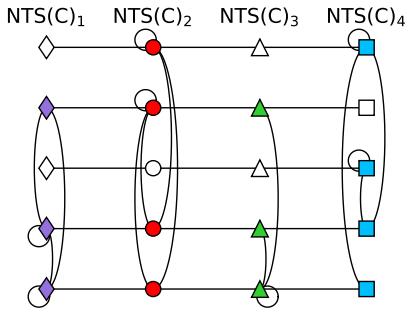

Figure 8: Representation of the multilayer network. The nodes of individual NTS(C)$_i$ networks are shown with the same node shape. Empty cells are shown in white color.

The nodes of the multilayer network are cells of the geographic area. All resulting NTS(C) networks consist of the same set of nodes. Since the NTS(C) networks have the same number of nodes, the MLN-NTS(C) network could also contain empty cells, i.e., cells that do not contain earthquakes and do not form connections with the rest of the cells within individual layers. However, each node represents a non-empty cell in at least one of the layers of the entire network.

By expanding the NTS(C) network into a multilayer network, the nodes representing the same cell are split into several sequentially connected nodes. In this manner, earthquakes located in the same cell are distributed over several cells with the same location depending on the time of their occurrence. Thus, earthquakes that occurred further apart in time no longer belong to the same node, even if they lie very close to each other in space.

We construct multilayer networks with $T = 1$, $T = 2$ and $T = 3$ layers[2].

5 Visualisation and comparison of networks

In this section, we describe the structure of the resulting networks, focusing on the number of components, the number of connections, and the connectivity of the networks.

[2]A multilayer network with one layer represents a NTS(C) network.

When generating networks according to the NTS(C) construction, we arrange earthquakes by the time of their occurrence and connect the cells corresponding to consecutive pairs of earthquakes. By doing so, none of the cells is disconnected from the rest of the network, and the network always consists of only one component (Figure 9: (a)-(c)).

In the MLN-NTS(C) construction, the time interval in which the network is generated is divided into two or three equally long subintervals (layers). Within each layer, we generate individual NTS(C) networks that are then connected to each other via identical cells between successive layers. The MLN-NTS(C) network also consists of only one component and does not contain isolated nodes (Figure 9: (d)-(i)). In time intervals in which a stronger earthquake occurs, the number of earthquakes and, thus, the number of connections in individual NTS(C) networks within the MLN-NTS(C) network increases. As a result, the cells within the layers are more densely connected than the cells between the layers (Figure 9: (e)-(i)).

In the VG(E) construction, where earthquakes are connected according to the "visibility" condition, each earthquake is always connected to its nearest neighbor in time. In the VG(C) network, instead of connections between earthquakes, we generate connections between the corresponding cells. The network, according to the VG(E) construction, contains all the connections contained in the NTS(C) network plus additional ones that arise due to the "visibility" condition between earthquakes. Thus, VG(C/E) networks also consist of only one component and do not contain isolated nodes.

Figure 10 ((a)-(f)) shows some of the networks generated by the VG(C/E) construction. It can be seen from Figure 10 ((a), (b), (d), (e)) that (stronger) earthquakes in the VG(E) network "shadow" the connections between some (weaker) earthquakes, which results in clearly visible groups in a network.

The "shadowing" effect is even more pronounced in the time intervals where a stronger earthquake occurs since such an earthquake triggers a large number of aftershocks of various magnitudes. Because the number of earthquakes with lower magnitudes is exponentially greater than the number of earthquakes with higher magnitudes (Gutenberg-Richter law, equation (1)), a lot of aftershocks have relatively low magnitudes. Since the occurrence of a strong earthquake results in a lot of aftershocks, there is a high probability that among the multitude of weaker earthquakes that lie close together in time, a stronger earthquake will also occur, thus breaking the connections between those weaker earthquakes. It is sufficient that the magnitude of the "stronger" earthquake is only slightly higher than the magnitude of "weaker" earthquakes.

The phenomenon of "shadowing" of connections is repeated at different magnitude values, where stronger earthquakes shadow the connections between weaker ones. Thus, weaker earthquakes that lie close together in time form a large number of groups that are connected to each other through earthquakes of higher magnitudes (Figure 10: (b), (e)).

When earthquakes are grouped into cells (VG(C) network), a spatial component is introduced into the network that groups nearby earthquakes into cells, regardless of their "visibility" to each other. Consequently, the branching of the network, which is the result of "visibility" between earthquakes, is somewhat destroyed. This is also the reason for the differences in behavior of the time series consisting of characteristics calculated from the networks according to the VG(E) and VG(C) constructions (section 6).

In the SVG(E) network, connections are generated similarly as in the VG(E) network, whereby the time-magnitude space in which the connections are generated is limited by a spatial window, the size of which is determined by the magnitude of the individual earthquakes. Due to the introduction of a spatial component, earthquakes that are adjacent in time are no longer necessarily connected to each other. It can be seen from Figure 10 ((g)-(i)) that networks generated according to the SVG(E) construction break up into several components, among which quite a few consist of individual nodes. In the component containing a larger number of nodes, the shape of the network is still very similar to the one obtained with the VG(E) network (Figure 10: (b), (e), (h)).

When earthquakes are grouped into cells, the branching of the SVG(E) network which is a result of the "visibility" between earthquakes is rather destroyed (similar as in the VG(C) network). When generating networks with increasingly larger cells, the components consist of an increasingly lower number of nodes, where the number of components remains approximately the same or decreases very slowly.

In the NTSW(E) construction, we generate two windows around each of the earthquakes - a spatial and a temporal window, the sizes of which are determined by the magnitude of the individual earthquakes. We connect each earthquake with all the earthquakes within the intersection of the two windows. In the NTSW(E) network, as well as in the SVG(E) network, earthquakes are connected only to those earthquakes that occured spatially close together.

However, the connection between earthquakes in the NTSW(E) network is also influenced by the temporal distance between earthquakes, while in the SVG(E) network, the connection between earthquakes is influenced by their "visibility" to each other. Thus, certain pairs of earthquakes in the NTSW(E) network are connected because they occurred close together in time, while in the SVG(E) network, these same pairs of earthquakes might not be connected because they might not "see" each other, and vice versa.

By merging nearby earthquakes into cells, we generate the NTSW(C) network. Figure 11 shows some of the networks generated by the NTSW(C/E) construction. The temporal and spatial windows belonging to earthquakes of higher magnitudes have a rather large temporal and spatial range (Figure 4). For this reason, NTSW(E) networks generated in time intervals in which a major earthquake occurs contain a higher number of connections than networks

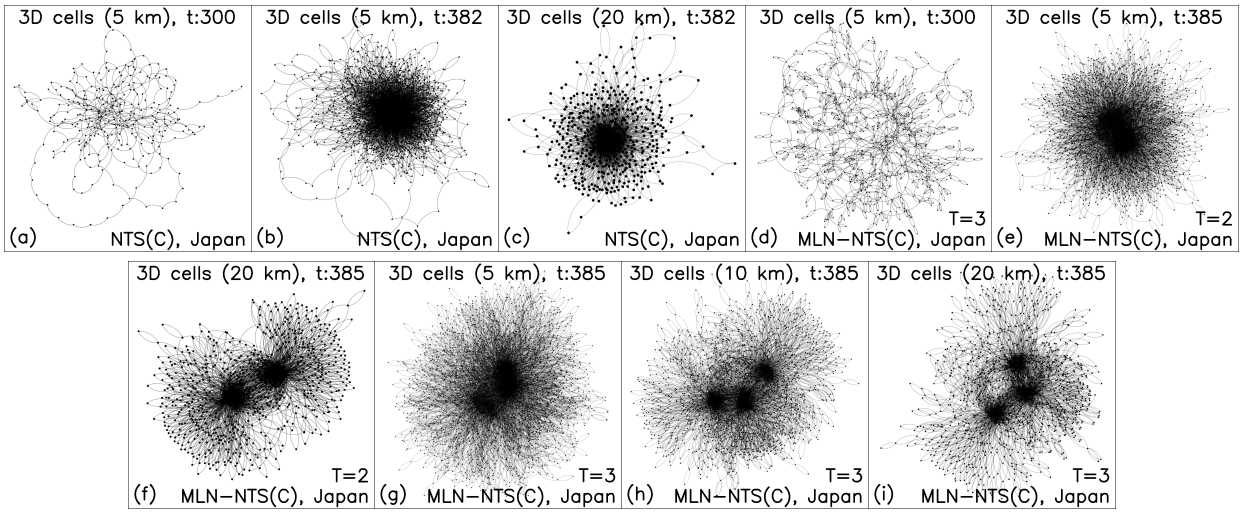

Figure 9: Some networks generated by the NTS(C) ((a)-(c)) and MLN-NTS(C) ((d)-(i)) constructions composed of cells of different sizes. The MLN-NTS(C) networks consist of $T = 2$ and $T = 3$ layers. Networks are generated from the Japanese catalog. The times given in the titles of the images represent the sequential number of a 10-day interval in which a stronger earthquake occurred ($t = 382$, $t = 385$) or the interval in which a stronger earthquake did not occur ($t = 300$). The networks in this Figure and in the rest of the Figures in this section were drawn with the program Gephi [27].

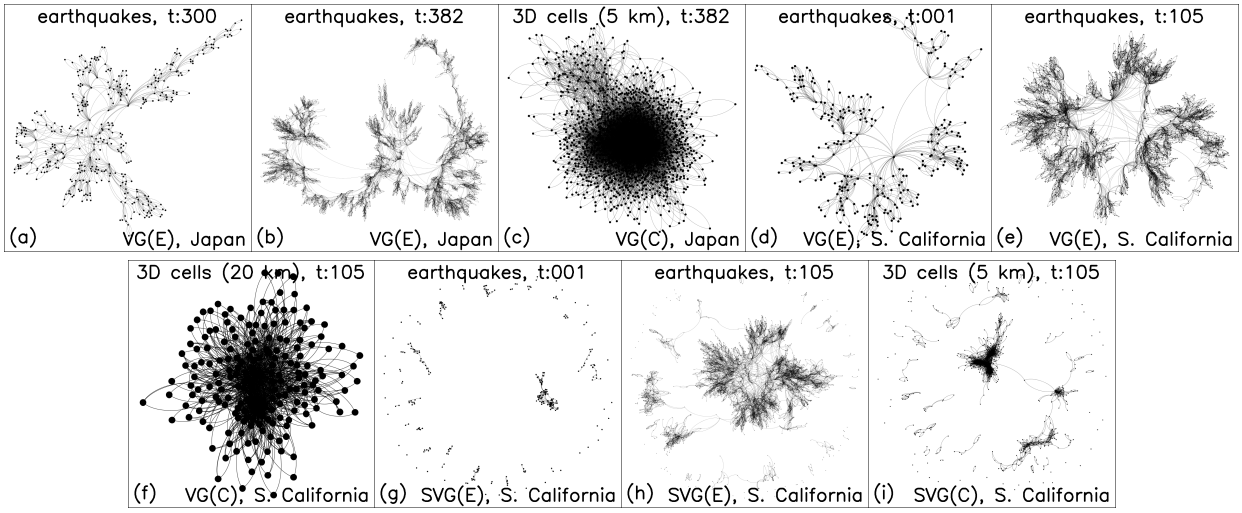

Figure 10: Some networks generated by the VG(C/E) ((a)-(f)) and SVG(C/E) ((g)-(i)) constructions, where the nodes in the VG(C) and SVG(C) networks are composed of cells of different sizes. Networks in (a)-(c) are generated from the Japanese catalog and the rest from the S. California catalog. The times given in the title of the images represent the sequential number of a 10-day (Japan) or 40-day (S. California) interval in which a stronger earthquake occurred ($t = 382$, $t = 105$) or the time interval in which a stronger earthquake did not occur ($t = 300$, $t = 001$).

generated by other constructions. The number of connections slowly decreases with the conversion of the NTSW(E) into the NTSW(C) network and with increasingly larger cell sizes in the NTSW(C) network (Figure 11).

When generating networks according to the NHTSW(E) construction, we connect pairs of earthquakes that have a sufficiently low value of n_{ij} calculated according to equation (4) so that the resulting networks have an average degree of $\langle k \rangle = 10$. In equation (4), n_{ij} depends on the time difference between the occurrence of two earthquakes, the distance between the hypocenters of these earthquakes, and on the magnitude of an earthquake that occurred first in the considered pair of earthquakes. Since the magnitude of the earthquake in equation (4) appears as a power of 10, it has a greater influence on the calculated value of n_{ij} compared to the product of time and distance.

The results (Figure 12) show that in the time intervals in which a stronger earthquake occurs, the distances (and times) between connected earthquakes are shorter on average than in the time intervals in which a stronger earthquake

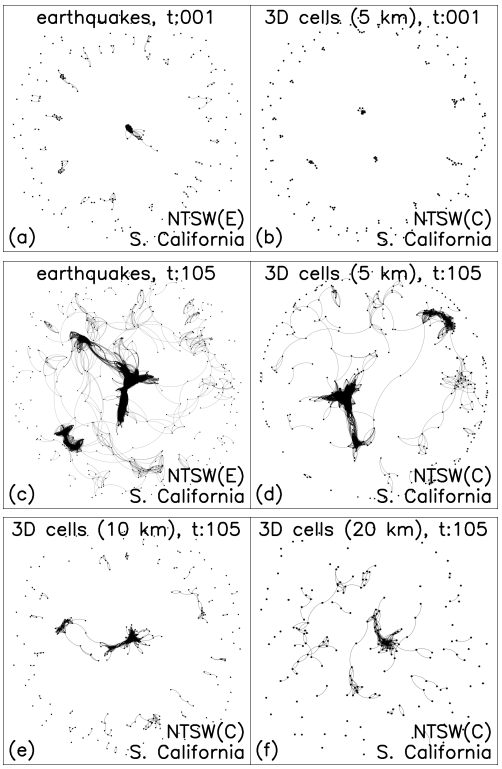

Figure 11: Some networks generated by the NTSW(E/C) construction, where the nodes consist of earthquakes or cells of different sizes. Networks are generated from the S. California catalog. The times given in the title of the images represent the sequential number of a 40-day interval in which a stronger earthquake occurred ($t = 105$) or the time interval in which a stronger earthquake did not occur ($t = 001$).

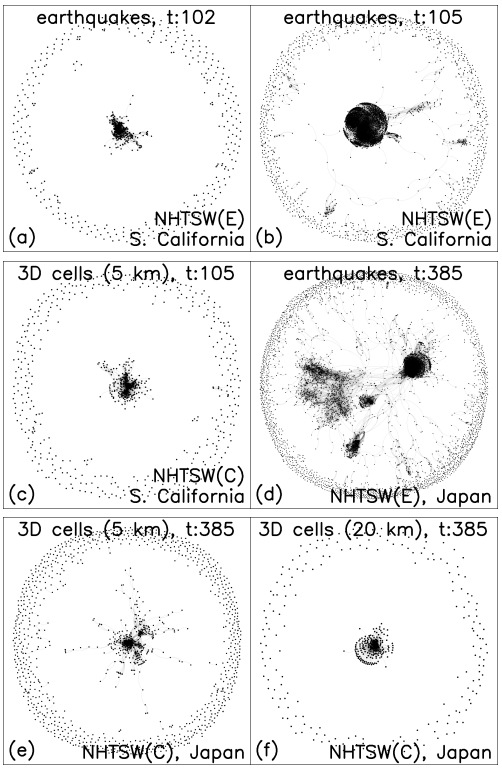

Figure 12: Some networks generated by the NHTSW(E/C) construction, where the nodes consist of earthquakes or cells of different sizes. Networks are generated from the Japanese ((d)-(f)) and the S. California catalog ((a)-(c)). The times given in the title of the images represent the sequential number of a 10-day (Japan) or 40-day (S. California) time interval in which a stronger earthquake occurred ($t = 105$, $t = 385$) or the time interval in which a stronger earthquake did not occur ($t = 102$).

did not occur. This is because the highest magnitude in the time interval determines the lowest value of n_{ij} (the highest correlation) among earthquakes connected in a network. Since we keep only $m = 5n$ of the most correlated connections, we ignore connections with n_{ij} above the specific threshold value that differs from network to network.

This threshold value depends on the lowest value of n_{ij} in the network and, consequently, on the highest magnitude in the time interval. In order for the other earthquakes (with magnitudes lower than the one of the strongest earthquake in the time interval) to be able to form connections in a network, their distance in time and space from the rest of the earthquakes needs to be comparably smaller than distances in time and space corresponding to the strongest earthquake. Otherwise, these weaker earthquakes cannot produce the low enough n_{ij} to form connections in a network.

This means that most of the connected earthquakes in the NHTSW(E) network lie very close in time and space. For this reason, a very rough transition between the NHTSW(E) and NHTSW(C) constructions can be observed in Figure 12 ((d)→(e)), where groups of connected earthquakes are suddenly contained in individual cells. In the NTSW(C/E) construction (Figure 11: (c)→(d)), in which the associated earthquakes are located within the spatial window, a transition from a network with earthquakes to a network with cells is not so pronounced since the spatial windows are relatively wide (Figure 4).

In the NCV(C) network, the time interval in which the network is generated is divided into T equally long time subintervals. For each of the cells, we generate a vector of length T. The elements of the vector represent some characteristic of the cell, calculated from the earthquakes that occurred within the cell in each of the time subintervals. Cells are connected based on the Pearson correlation coefficient between pairs of vectors.

When generating the NCV(C) network, we also analyze the vectors belonging to each cell. From the analysis of vectors we observe that the obtained vectors consist of almost only zero values. In the majority of the vectors, only one of the elements is non-zero. This means that the earthquakes in most of the cells occurred within the same time subinterval.

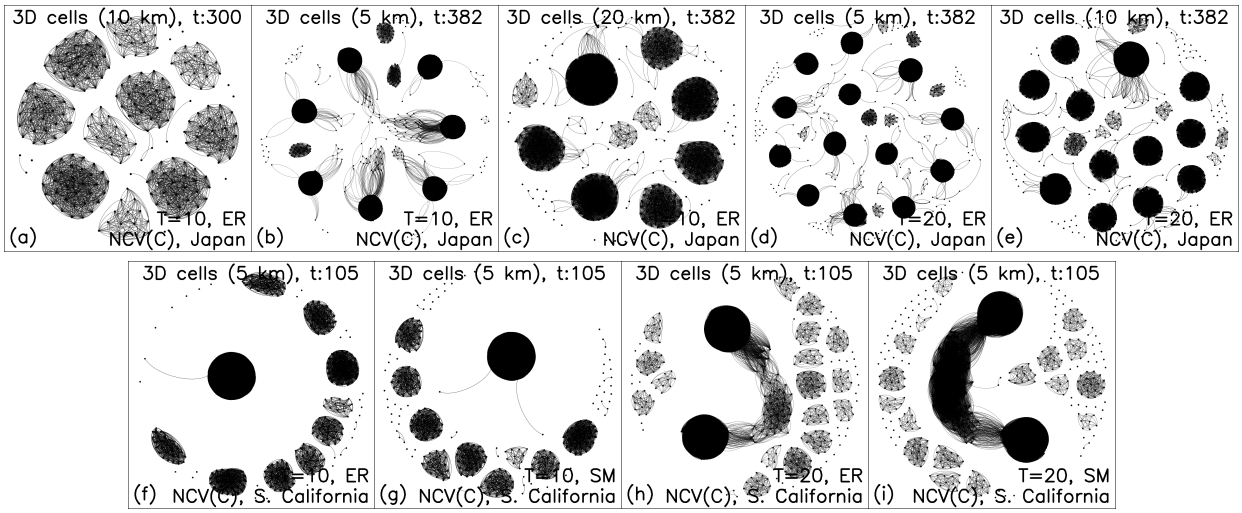

Figure 13: Some networks generated by the NCV(C) construction consisting of cells of different sizes. Networks are generated from the Japanese ((a)-(e)) and S. California catalogs ((f)-(i)). The times given in the title of the images represent the sequential number of a 10-day (Japanese) or 40-day (S. California) time interval in which a stronger earthquake occurred ($t = 105$, $t = 382$) or the time interval in which the stronger earthquake did not occur ($t = 300$). In the images, the abbreviation SM indicates networks where the characteristic used to calculate elements of the vectors is the sum of earthquake magnitudes, and the abbreviation ER indicates networks where the characteristic is the amount of energy released by earthquakes.

As a result, when calculating the Pearson correlation coefficient, we mostly consider two types of pairs of vectors – those that contain a non-zero element at the same position of the vector and those that contain a non-zero element at different position of the vector, where all other elements in the vector are equal to 0. In the first case, the value of the Pearson correlation coefficient corresponding to a given pair of vectors is $r = 1$, while in the second case, it is $r = -1/(T-1)$. This is true regardless of the value of the non-zero element (only positive values are considered), which can be deduced from the equation (5). Thus, most pairs of cells are connected by the Pearson correlation value of $r = -1/(T-1)$. However, these connections are not present in the network since $|r| = |-1/(T-1)| \leq 0.95$ for $T > 2$.

Figure 13 shows that NCV(C) networks consist of well-defined groups. These groups are the result of connections between cells with vectors composed of only one non-zero element. The non-zero element in all vectors in the same group appears at the same position. The number of well-defined groups in a network is equal to the number of elements in vectors belonging to the cells. Cell vectors in one group differ from cell vectors in another group in the position of the non-zero element. Pairs of cells in which the non-zero element appears at non-overlapping positions are not connected to each other.

Well-defined groups in the network are, in some cases, connected to each other (Figure 13: (b), (d), (h), (i)). The value of $|r| > 0.95$ can also be obtained, for example, from a pair of vectors where one of the vectors contains only one non-zero element and the other contains several non-zero elements. In this case, the non-zero component in the first vector must match one of the non-zero components in the second vector[3]. Thus, cells corresponding to vectors with several non-zero elements can also be part of individual well-defined groups.

Vectors that contain more non-zero elements can be connected to other vectors that also contain several non-zero elements, but are not connected in well-defined groups. In this way, shorter or longer paths can emerge in the network, starting in individual groups and connecting groups to each other. Whether the network will contain such paths depends on the activity of the area, the distribution of earthquakes in the area, and the size of the cells.

In the time intervals in which a stronger earthquake occurs, some of the groups are more densely connected than others (Figure 13: (b)-(i)). This is due to the fact that the stronger earthquake did not occur at the beginning of the time interval in which the network is generated but later. If a stronger earthquake occurs in the i-th subinterval, groups consisting of vectors containing a non-zero element at $j \geq i$-th index will be more densely connected than those containing a non-zero element at $j < i$-th index.

For example, in the Japanese catalog (at $t = 382$), the stronger earthquake in the network with $T = 10$ subintervals occurs in the 4-th subinterval and in the network with $T = 20$ subintervals it occurs in the 8-th subinterval. Therefore, only 7 out of 10 (Figure 13: (b), (c)) and only 13 out of 20 (Figure 13: (d), (e)) groups in the network are

[3]The value of r between the two described vectors also depends on the magnitude of values in the vector, which contains several non-zero elements.

more densely connected. Similarly, in the S. California catalog (at $t = 105$), a stronger earthquake occurs in the last ($T = 10$) or penultimate ($T = 20$) subinterval, which contributes to only one (Figure 13: (f), (g)) or two (Figure 13: (h), (i)) more densely connected groups in the network.

6 Time series

In this section, we present and describe some of the generated time series, limiting results to time series obtained from distances between nodes (average shortest path) and from the characterisation of the community of nodes (modularity). In the following equations n denotes the number of nodes, m denotes the number of edges, V denotes the set of vertices and $\mathcal{C}$ denotes the set of connected components in a network. Notations v_i and v_j denote nodes i and j, notations k_i and k_j denote degrees of nodes i and j, and n_c denotes the number of nodes in component c.

The average shortest path $\langle d \rangle$ [28] is calculated using the equation

$$\langle d \rangle = \frac{\sum_{v_i, v_j \in V, v_i \neq v_j} d(v_i, v_j)}{n(n-1)}. \tag{6}$$

In the case of a disconnected network, the average shortest path is calculated for the largest connected component in a network ($\langle d_{LCC} \rangle$). Time series obtained in such a way are compared to time series of the average shortest path calculated for each connected component, where values are combined using a weighted average. The weight represents the number of nodes in each connected component, according to the equation $\langle d \rangle = \frac{1}{n} \sum_{c \in \mathcal{C}} n_c \langle d(c) \rangle$.

Modularity Q [29] is defined with the equation

$$Q = \frac{1}{2m} \sum_{v_i, v_j \in V} \left(A_{ij} - \frac{k_i k_j}{2m} \right) \delta(s_i, s_j), \tag{7}$$

where s_i and s_j represent groups of nodes in which nodes i and j are located. Only pairs of nodes that are in the same group contribute to the value of the sum. Factor $A_{ij} - \frac{k_i k_j}{2m}$ represents the difference between the number of connections between nodes i and j in the network and the number of connections between nodes i and j in a random network model with predefined degrees of nodes (configuration model) [30]. Modularity is defined in the interval $[-1, 1]$, where high values represent networks with well-defined communities of nodes, i.e. densely connected groups of nodes and a small number of links between groups. Groups of nodes are obtained using the Leiden algorithm [31].

Figures 14, 15 (top two images), 17, 18, and 19 (top image) show the resulting time series of the average shortest path for some of the networks. It can be seen from Figure 14 that values of the average shortest path for the NTS(C), MLN-NTS(C), VG(C), and NHTSW(C/E) networks in time intervals in which a stronger earthquake occurs, suddenly drop. As a consequence of a strong earthquake, a large number of earthquakes occur in the cell of an earthquake and the surrounding cells, increasing the number of connections in that part of the network. As a result, "shortcuts" are created, and thus, the value of the average shortest path decreases[4].

In time intervals with low seismicity, the SVG(C/E) and NTSW(C/E) networks are composed of several smaller components (Figure 10: (g) and 11: (b)), resulting in low values of the average shortest path (Figure 15). In time intervals in which a larger earthquake occurs, some of the components connect with each other (Figure 10: (h)-(i) and 11: (d)-(f)); therefore, the average shortest path in the network increases (Figure 15). Figure 15 shows that the increase of the average shortest path for these networks mostly happens a few intervals after the vertical line; in the 385th interval, when the largest earthquake occurs.

In the VG(E) network, the sudden jump in values of the average shortest path during a strong earthquake (Figure 14) is due to the hierarchical structure of the network, which results in long paths from one part of the network to the other. In the VG(C) network, this hierarchical structure is destroyed, as earthquakes that are spatially close to each other get grouped into cells, regardless of their distance in the network, consequently shortening the paths in the network.

In the MLN-NTS(C) network, the introduction of layers causes identical cells to split into multiple nodes, which lengthens paths in the network. As a result, the average shortest path increases as the number of layers increases (Figure 19).

In the case of the NCV(C) network, which in the time intervals with low seismicity, consists of several well-connected separate components (Figure 13: (a)), it may happen that components connect to each other during a larger earthquake. This leads to an increase in the value of the average shortest path (Figure 17). Since the connectivity between well-defined groups in the NCV(C) network depends on the activity and the distribution of earthquakes in the area, one cannot know with certainty whether the value of the average shortest path will increase or remain the same as in time intervals before a stronger earthquake.

[4] A sudden change in values of the average shortest path is in the case of the Japanese catalog less visible for the NHTSW(C/E) network (Figure 14), however it is clearly visible in some of the other catalogs.

[5] The vertical lines actually indicate the time interval in which the earliest earthquake in a group of stronger earthquakes containing the strongest earthquake in the catalog occurs. For example, in the Japanese catalog, the strongest earthquake with $M = 6.8$ occurs in the 385th interval. However, a few weaker but still very strong earthquakes happen beforehand, starting in the interval 382 ($M = 6.4$, $M = 6.0$). If we consider only the interval 385 and observe the changes in time series in the preceding intervals, it seems as if the event can be predicted since noticeable changes in the time series occur already in time interval 382. The vertical line in the Japanese case therefore mark the 382th interval. Similarly, in the S. California catalog, the strongest earthquake with $M = 7.3$ occurs in the 105th interval. However, noticeable changes in the time series happen already in the 104th interval when the earthquake with $M = 6.1$ occurs.

[6] Since the NTSW(E) networks contain an immense number of con-

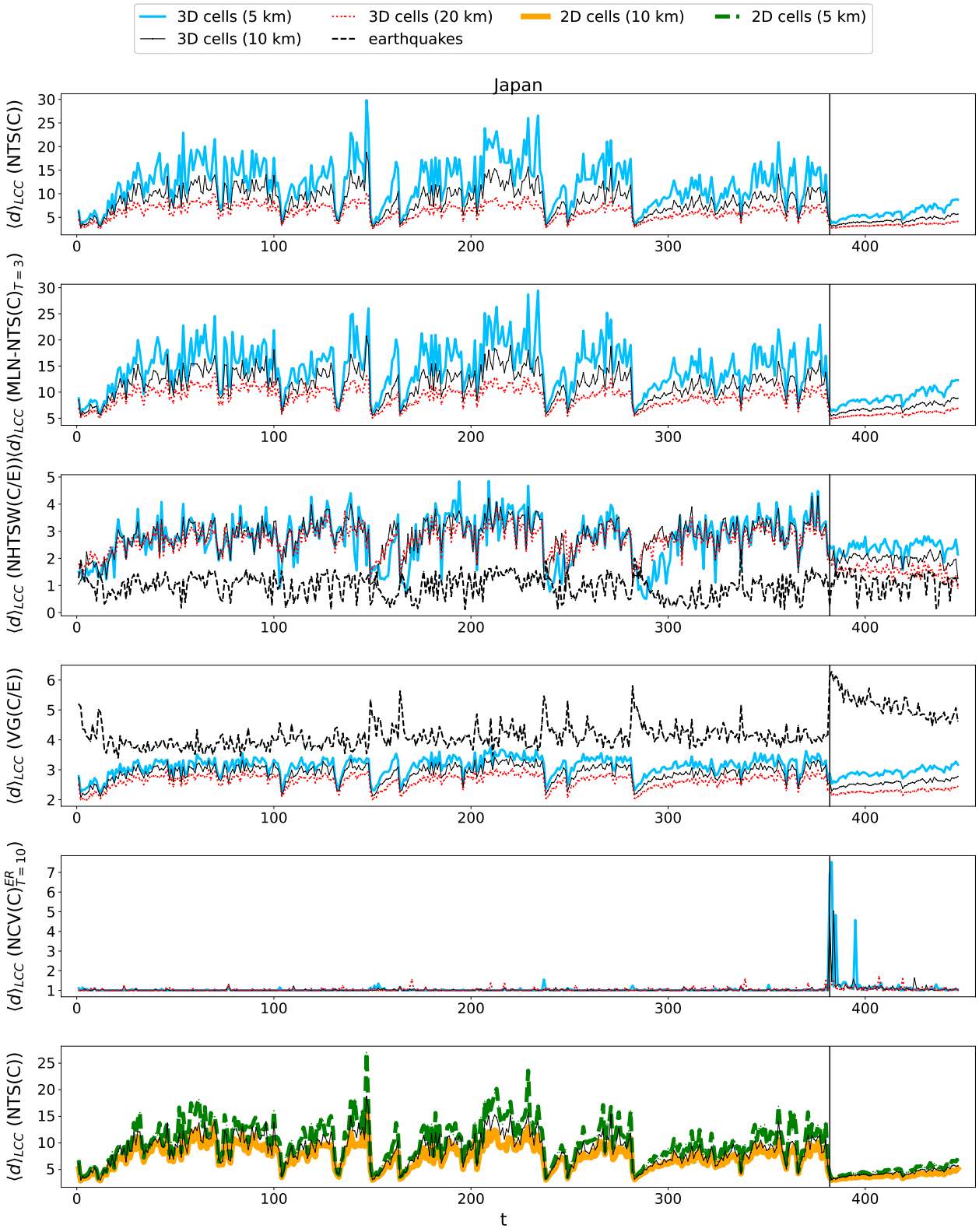

Figure 14: Time series of the average shortest path for the NTS(C), MLN-NTS(C), NHTSW(C/E), VG(C/E), and NCV(C) constructions generated from the Japanese catalog. The vertical lines indicate the intervals in which the strongest earthquake in the catalog occurs[5].

nections (section 5), which significantly increases the computational time of algorithms, time series composed of characteristics of the NTSW(E)

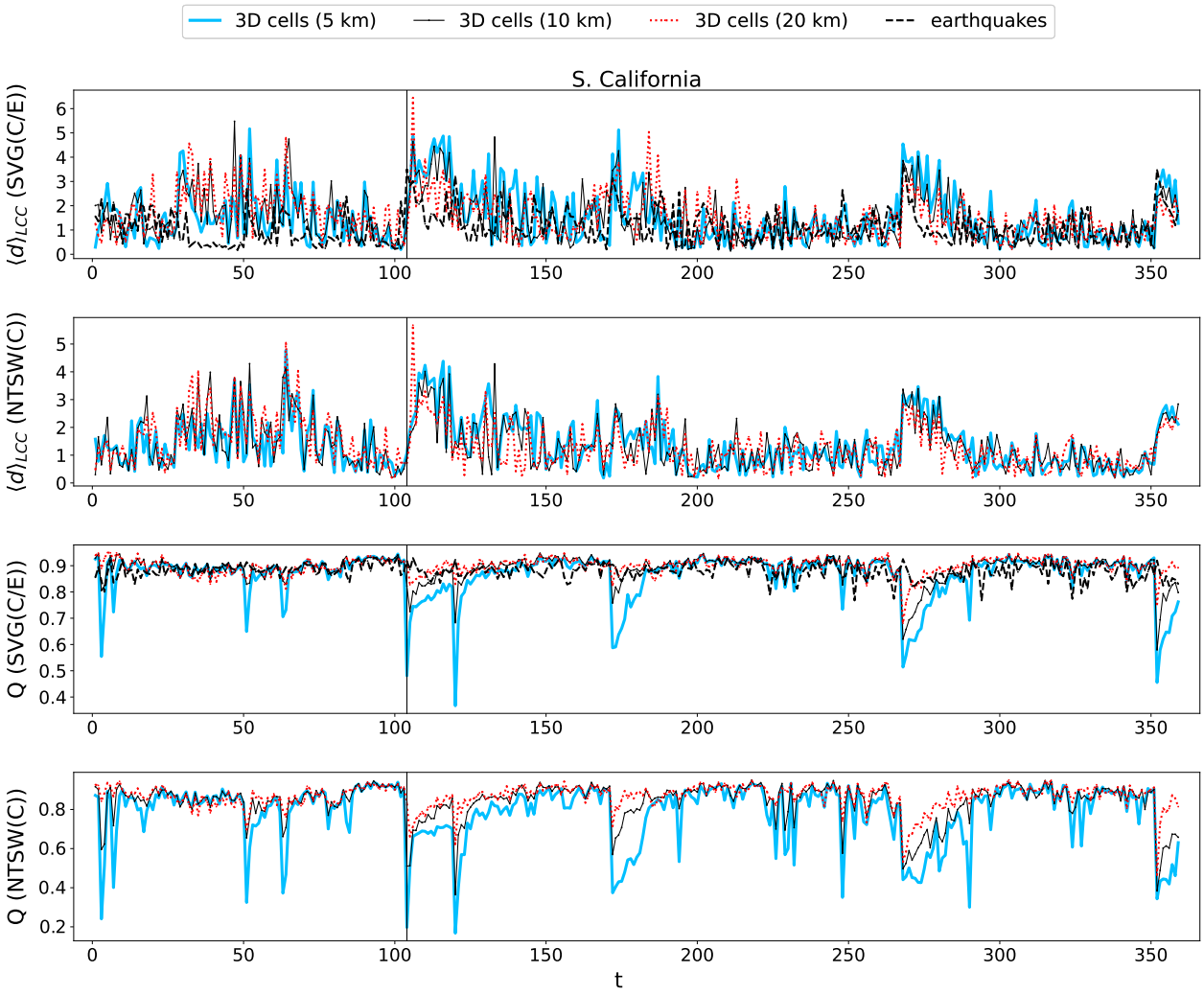

Figure 15: Time series of the average shortest path (top two images) and modularity (bottom two images) for the SVG(C/E) and NTSW(C)[6] constructions generated from the S. California catalog. The vertical lines indicate the intervals in which the strongest earthquake in the catalog occurs[5].

For time series of the NTS(C), VG(C), and MLN-NTS(C) networks we observe that values of the average shortest path obtained from networks consisting of larger cells are generally lower than values of the time series obtained from networks consisting of smaller cells. This is due to the fact that networks composed of larger cells are smaller, which makes the paths between nodes shorter than in networks composed of smaller cells. Similar results can be observed comparing time series obtained from networks consisting of 2D and 3D cells, where it seems that 2D cells represent only a larger representative of the corresponding 3D cells. For example, values of time series for the NTS(C) networks composed of 2D cells of size 10 km are consistently lower than values of these series where networks are composed of 3D cells of the same size (Figure 14: bottom image).

Such a difference in results between larger and smaller cells, however, is not repeated for the NTSW(C), SVG(C), and NHTSW(C) networks, in which a spatial component is introduced. In time intervals with low seismicity these networks consist of many very small components that do not change much with the conversion from smaller to larger nodes (Figure 11: (a), (b)). Only in time intervals with higher seismicity, where the component containing the larger earthquake as well as the components connected with it grow in size, some differences can be observed when comparing networks composed of different cell sizes (Figure 11: (d), (e), (f)).

Time series obtained from the Italian catalog are smoother than those obtained from the other catalogs. Since the time intervals of the Italian catalog are longer and overlap with each other, differences in smoothness of the time

network are not generated.

[7] Since time intervals of the Italian catalog, which are 150 days long, overlap by 50 days, the strongest earthquake in the catalog occurs in three consecutive time intervals represented by the shaded area.

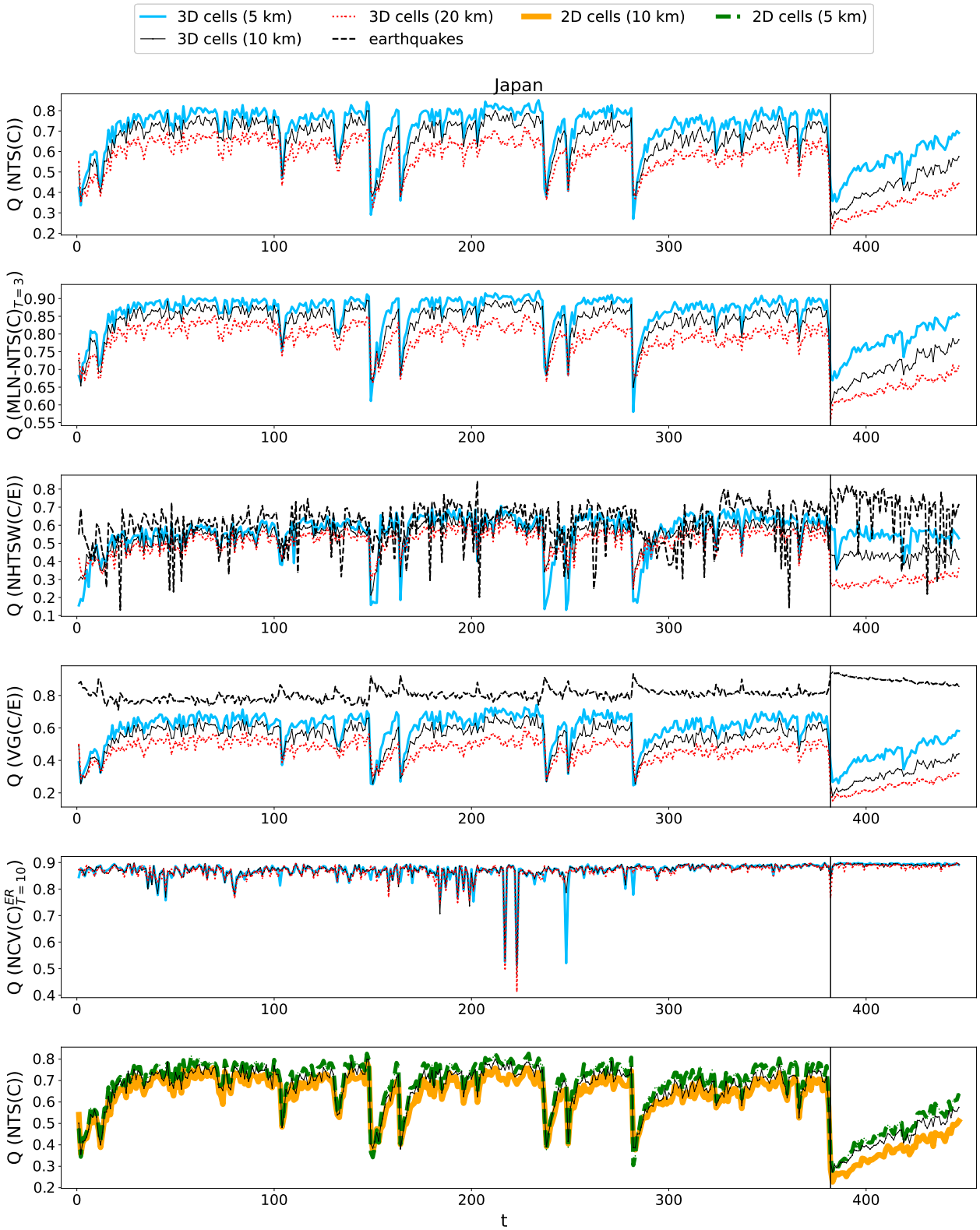

Figure 16: Time series of modularity for the NTS(C), MLN-NTS(C), NHTSW(C/E), VG(C/E), and NCV(C) constructions generated from the Japanese catalog. The vertical lines indicate the intervals in which the strongest earthquake in the catalog occurs[5].

series between different catalogs are not surprising. In addition, slight differences can also be observed between the time series composed of California and Japanese catalogs, where time series of California catalogs are a bit smoother.

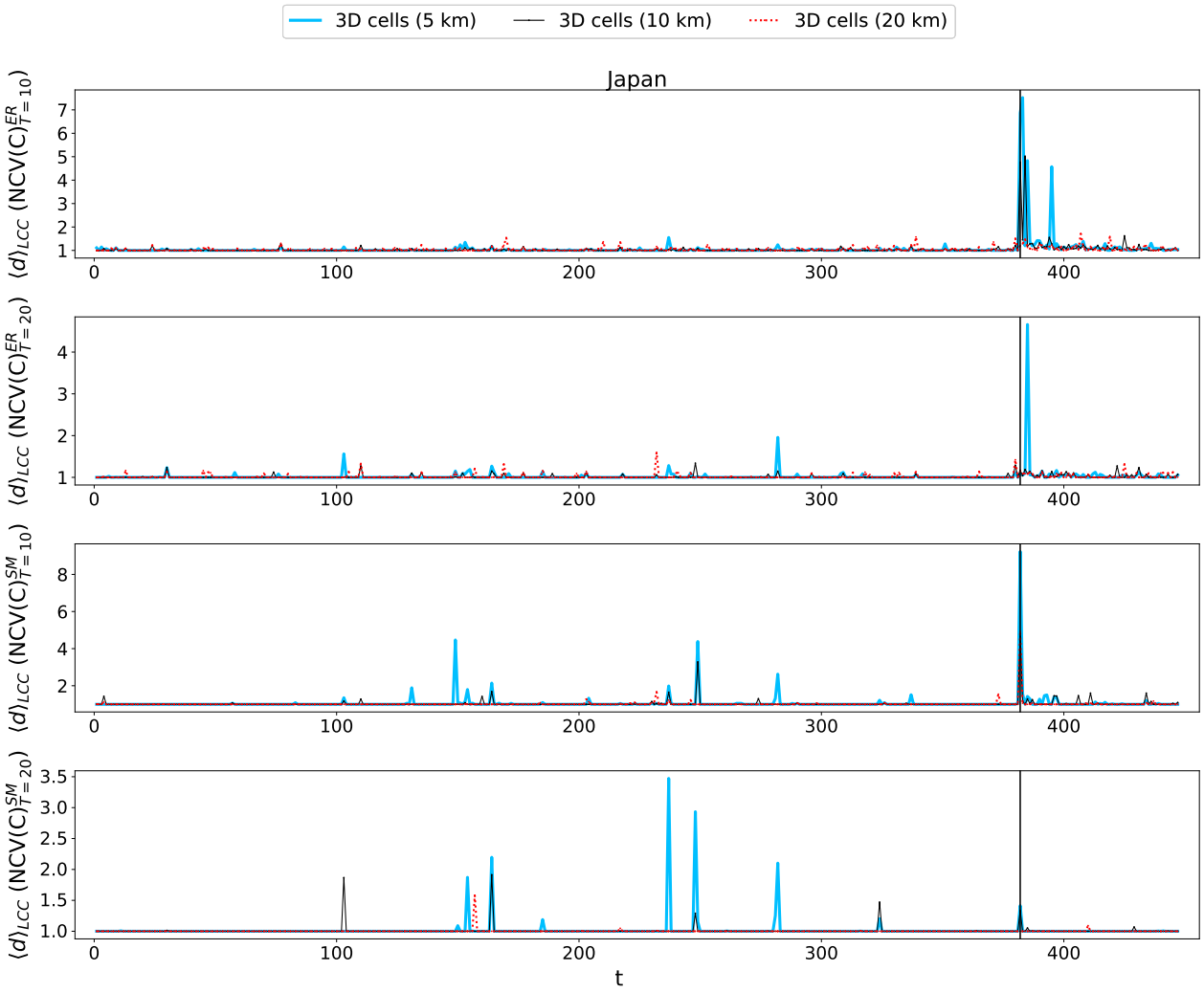

Figure 17: Time series of the average shortest path for the NCV(C) construction generated from the Japanese catalog. The vertical lines indicate the intervals in which the strongest earthquake in the catalog occurs[5].

This is again most likely due to the difference in length of the time intervals between catalogs.

In networks consisting of several components, averaging the value of the average shortest path across all components results in a smoother variation of the time series versus using the average shortest path of the largest component in the network.

In the case of the time series consisting of modularity of the generated networks, we again observe that values of most of the time series drop sharply in the time intervals in which a stronger earthquake occurs (Figure 15: bottom two images and 16). In time intervals with low seismicity, networks consist of well-defined smaller local groups. When a larger earthquake occurs, the part of the network containing the earthquake is connected to the rest of the network through a greater number of links. As a result, the groups are no longer clearly separated from each other.

Networks consisting of larger cells contain a smaller number of connections, which means that groups in such networks are generally less well-defined. For this reason, the value of modularity in the NTS(C), VG(C), and MLNNTS(C) networks with larger cells is generally lower than in networks with smaller cells (Figure 16). This, however, does not apply for networks compiled with the spatial component taken into account (NTSW(C), SVG(C), NHTSW(C)).

In the case of the VG(E) network, the value of modularity increases in the intervals in which a larger earthquake occurs, which is a consequence of the branching of the network (Figure 16).

In time intervals with low seismicity, the value of modularity in the NCV(C) network is close to 1. When a stronger earthquake occurs, the modularity value could decrease or remain similar to the values in the time intervals when no stronger earthquake occurs. This is again due to the fact that the formation of shorter or longer paths that start in individual groups depends on the distribution of earthquakes and the activity of the area.

Figure 18: Time series of the average shortest path for the NTS(C) construction generated from the Japanese, Italian, S. California, and N. California catalogs. The vertical lines and the shaded area[7] indicate the intervals in which the strongest earthquake in the catalog occurs[5].

In time intervals in which a larger earthquake did not occur, the values of obtained time series, regardless of the characteristic they are composed of, fluctuate around the value corresponding to the background seismicity. In case of a stronger earthquake, the values of the series change suddenly. Then, as long as the aftershock series of the given earthquake is present, values are rising or falling towards their reference values.

We also notice that the values in the time series after a larger earthquake take longer to approach the reference values than the values in the time series after a slightly smaller but still strong earthquake. The reason is that a stronger earthquake triggers a large number of connections, causing the aftershock series to last for a longer period of time.

7 Discussion

We analyze changes in seismicity in consecutive time windows covering the span of multiple years. In each time window, we build a network according to seven different models: the NTS(C), NTSW(C/E), NHTSW(C/E), VG(C/E), SVG(C/E), NCV(C), and MLN-NTS(C). The data for seismic activity is obtained from Japanese, Italian, Southern, and Northern California catalogs.

Nodes of the NTSW(C/E), NHTSW(C/E), VG(C/E), and SVG(C/E) networks are represented by earthquakes or smaller blocks of geographic area (cells), while nodes of the NTS(C), MLN-NTS(C), and NCV(C) networks are represented only by cells. The node type and node size are free parameters in these networks. The MLN-NTS(C) and NCV(C) networks are constructed with additional parameters, namely, the number of layers in the MLN-NTS(C) network, and the characteristic of a cell and the length of cell vectors in the NCV(C) network.

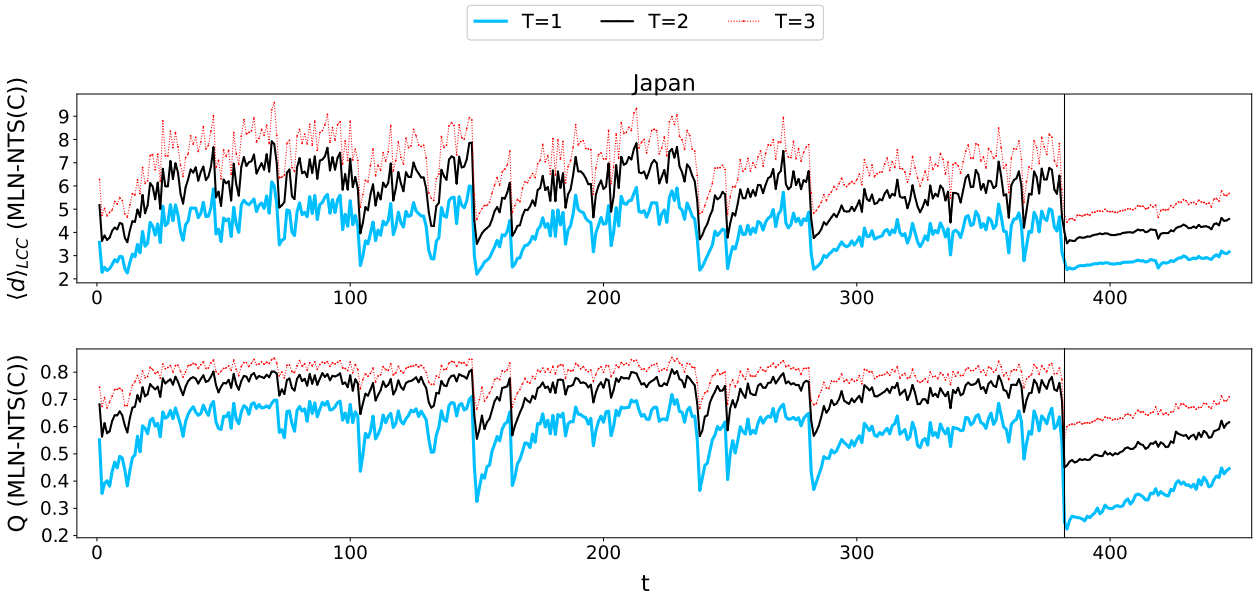

Figure 19: Time series of the average shortest path and modularity for the MLN-NTS(C) construction generated from the Japanese catalog. The vertical lines indicate the intervals in which the strongest earthquake in the catalog occurs[5].

The SVG(C/E) network represents a new network model introduced in this paper and is composed as a combination of the VG(C/E) and NTSW(C/E) network.

We use named network models, also changing the parameters to generate several time series that consist of values of the average shortest path and modularity of obtained networks. The investigation of the changes in acquired time series is mainly concerned with answering two posed questions. Firstly, can time series constructed from these networks be used to determine the time intervals in which the seismic activity increases, and secondly, can changes in time series serve as a predictor of an impending earthquake.

This study constitutes a preliminary analysis to show that certain traits can consistently be observed with these networks regardless of the node size and selected seismic catalog. Analysis is focused on the time evolution of networks and the resulting time series where a larger number of time intervals is used compared to studies listed in the Related works section, which focus primarily on the properties of a single or a few networks created from the catalog. The results of this paper and the related papers are summed up in Table A.1.

From the analysis and comparison of the obtained networks, we observe that all networks, except the NVC(C) network, are structurally built so that the corresponding time series describe the changes in the seismic activity in individual time intervals relatively well. In the time intervals with higher seismicity, networks become more densely connected, which leads to sudden changes in the values of the associated time series.

When generating NCV(C) networks, we use vectors of two different sizes where vectors are constructed using two different cell characteristics. Results show that a similar structure is obtained for all four types of networks. Because the structure of the NCV(C) network in time intervals with higher seismicity depends on the distribution of earthquakes and the activity of the area, this network produces time series with unreliable changes.

Time series generated using the MLN-NTS(C) network change similarly regardless of the number of layers in the network. Although, the MLN-NTS(C) networks consisting of multiple layers have higher values of the average shortest path and modularity than those consisting of fewer layers.

The SVG(C/E) network structurally represents characteristics of both the VG(C/E) and NTSW(C/E) network. In the SVG(E) network, we observe similar branching behavior as in the VG(E) network, where the split of the network into several components that connect to each other in time intervals with increased seismicity is the influence of spatial component in the NTSW(C/E) network.

When generating networks, we use nodes of various sizes, from the hypocenters of individual earthquakes, which are point size, up to 20 km cells that are shaped as cubes or square prisms. The results show that visible changes in the time series occur regardless of the size of the node. However, in time intervals with higher seismicity clearer changes in the time series can be obtained using smaller nodes, although smaller nodes simultaneously contribute to greater fluctuations of the whole time series. From the network visualizations itself, a network with increased seismic activity is easier to recognize using smaller nodes.

The sudden changes in time series do not happen before the time interval of a bigger earthquake; thus, observing only changes in the time series, one cannot conclude beforehand when a bigger earthquake is about to occur. There-

fore, the results of the study are not directly applicable for predicting the next time interval containing strong seismic activity. However, since noticeable changes happen in the time series when a larger earthquake occurs, further analysis is needed to test whether the use of some machine learning model that can recognize such patterns would be of help in predicting a sudden change in the time series using the previous values in the series.

An example of such a model are recurrent neural networks (RNNs) and their improved versions [32]. Recurrent neural networks are used to predict sequential data or time series, where the output from the previous step is reused as part of the input to the current step. RNNs can be improved into grids with long short-term memory (LSTM), which can learn long-term dependencies and thus recognize and remember important information in the previous and more distant values of the series and discard the information that is not important for the prediction.

In case some machine learning model could forecast the value of the time interval containing a larger earthquake, these predictions could be directly used to warn people about an upcoming earthquake and evacuate the area.

Networks generated at individual time intervals consist of earthquake data over the entire catalog area. In practice, it would be highly beneficial to conduct the analysis also on smaller parts of the area, which could lead to better model applicability. This approach would localize inter-earthquake effects since earthquakes outside the area would not affect those in the selected area. Subsequently, impacting the structure of the generated networks and time series, and potentially improving the predictability of seismic events.

Time series presented in the paper consist of values of the average shortest path and modularity. However, the study was done also on some other characteristics related to the global properties of networks, e.g., diameter and mixing coefficient, and characteristics related to the properties of individual nodes, e.g., clustering coefficient and closeness centrality. Nonetheless, all networks are constructed from data over the entire catalog area, limited only in time by the bounds of the corresponding time intervals.

Time series composed of characteristics related to the properties of individual nodes are constructed by first selecting a stronger earthquake in the catalog and determining the cell the earthquake is located in. Then, for each network in the series, the sum of the characteristic values of the determined cell and its surrounding cells is calculated. To determine the surrounding cells several different radii values are used. Lastly, the calculated sum values are assembled into the time series. The results again show that gained time series describe the changes in seismicity relatively well but still do not show any specific changes before the occurrence of a stronger earthquake.

We notice that time series consisting of data from different catalogs differ in smoothness, which is most likely due to the difference in lengths and overlaps of time intervals representing time points of generated series. Otherwise, networks generated using the data from different catalogs and the corresponding time series are similar to each other. Furthermore, the analysis was done on two additional datasets, a Greek [33] and another Japanese [16] catalog, where we also observe that the change in seismicity during a larger earthquake is reflected in the associated time series.

To generate comparable networks between catalogs, we adjust the length of the time intervals for each catalog according to the number of data in the catalog and the length of the catalog. As a result, time series composed of data from the same catalog consist of intervals of only one length. To attain more comprehensive results, further investigation needs to be done on the impact of length of time intervals and the impact of regional differences on the efficacy of network models.

The influence of these parameters can be obtained by expending the study where intervals of different lengths are constructed for each catalog. These intervals can be used as new time points for reconstruction of the time series. Thorough investigation should be done on analysis of smoothness of reconstructed time series for each region separately and on examination of these time series between regions at equally long intervals. Nevertheless, because the catalogs contain a different number of data, constructing equally long intervals for all catalogs could lead to the incomparability of the generated networks between different regions.

To make the study more robust with respect to the node size, one could generate networks consisting of cells of many sizes and analyze which size provides the best results in determining the time of a larger earthquake for each network model, length of the time intervals, and region separately. A similar analysis could also be performed on datasets from which aftershocks have been removed so that the remaining earthquakes are independent of each other. This would affect the structure of the generated networks, as most models assume dependency between earthquakes, where the occurrence of an earthquake triggers subsequent earthquakes. A comparison of results of these studies could provide new insights into the relationships and correlations between earthquakes.

Acknowledgements

This work has been supported in part by Slovenian Research and Innovation Agency ARIS under the program P5-0168.

References

[1] Stein Seth and Michel Wysession. An introduction to seismology, earthquakes, and earth structure. Blackwell. Chap. 3. 158. 2003. https://doi.org/10.1063/1.1629009.

[2] The Seismology and Natural Hazards Divisions of the European Geosciences Union (EGU). https://www.egu.eu/sm/can-we-predict-earthquakes/ (visited on July 25, 2020).

[3] Uprava Republike Slovenije za zaščito in reševanje, Izpostava Koper. Ocena potresne ogroženosti obalne regije. Tech. rep. 2019. 2019.

[4] Yan Y. Kagan and David D. Jackson. Probabilistic forecasting of earthquakes. Geophysical Journal International 143 (2): 438–453. Nov. 2000. https://doi.org/10.1046/j.1365-246X.2000.01267.x.

[5] Soghra Rezaei et al. The earthquakes network: Retrieving the empirical seismological laws. Physica A: Statistical Mechanics and its Applications 471: 80–87. Apr. 2017. https://doi.org/10.1016/j.physa.2016.12.003.

[6] Sumiyoshi Abe and Norikazu Suzuki. Scale-Free Network of Earthquakes. Europhysics Letters 65 (4): 581–586. 2004. https://doi.org/10.1209/epl/i2003-10108-1.

[7] Xuan He et al. Earthquake networks based on space–time influence domain. Physica A: Statistical Mechanics and its Applications 407: 175–184. Aug. 2014. https://doi.org/10.1016/j.physa.2014.03.093.

[8] Marco Baiesi and Maya Paczuski. Scale-free networks of earthquakes and aftershocks. Phys. Rev. E 69. 2004. https://doi.org/10.1103/physreve.69.066106.

[9] Luciano Telesca and Michele Lovallo. Analysis of seismic sequences by using the method of visibility graph. Europhysics Letters 97. Feb. 2012. https://doi.org/10.1209/0295-5075/97/50002.

[10] Joel N. Tenenbaum, Shlomo Havlin, and H. Eugene Stanley. Earthquake networks based on similar activity patterns. Phys. Rev. E 86. 2012. https://doi.org/10.1103/physreve.86.046107.

[11] Nastaran Lotfi, Amir Hossein Darooneh, and Francisco Aparecido Rodrigues. Centrality in earthquake multiplex networks. Chaos 28. 2018. https://doi.org/10.1063/1.5001469.

[12] Southern California Earthquake Data Center. https://scedc.caltech.edu/eq-catalogs/ (visited on June 1, 2020).

[13] High Sensitivity Seismograph Network Laboratory. http://www.hinet.bosai.go.jp/topics/JUICE/ (visited on June 1, 2020).

[14] Sumiyoshi Abe and Norikazu Suzuki. Dynamical evolution of clustering in complex network of earthquakes. The European Physical Journal B - Condensed Matter and Complex Systems 59: 93–97. Sept. 2007. https://doi.org/10.1140/epjb/e2007-00259-3.

[15] Insitituto nazionale di geofisica e vulcanologia. http://iside.rm.ingv.it/ (visited on June 1, 2020).

[16] Earthquake and Volcano Information Center. http://wwweic.eri.u-tokyo.ac.jp/CATALOG/junec/ (visited on June 1, 2020).

[17] Northern California Earthquake Data Center. https://www.ncedc.org/ncedc/catalog-search.html (visited on June 1, 2020).

[18] C. Godano, E. Lippiello, and L. de Arcangelis. Variability of the b value in the Gutenberg–Richter distribution. Geophysical Journal International 199 (3): 1765–1771. Oct. 2014. https://doi.org/10.1093/gji/ggu359.

[19] J. Wang et al. New Evidence and Perspective to the Poisson Process and Earthquake Temporal Distribution from 55,000 Events around Taiwan since 1900. Natural Hazards Review 15: 38–47. Feb. 2014. https://doi.org/10.1061/(asce)nh.1527-6996.0000110.

[20] J. Greenhough and Ian Main. A Poisson model for earthquake frequency uncertainties in seismic hazard analysis. Geophysical Research Letters 35. July 2008. https://doi.org/10.1029/2008gl035353.

[21] Sumiyoshi Abe and Norikazu Suzuki. Main shocks and evolution of complex earthquake networks. en. Brazilian Journal of Physics 39: 428–430. Aug. 2009. https://doi.org/10.1590/s0103-97332009000400014.

[22] Don W. Steeples and Dan D. Steeples. Far-field aftershocks of the 1906 earthquake. Bulletin of the Seismological Society of America 86 (4): 921–924. Aug. 1996. https://doi.org/10.1785/bssa0860040921.

[23] J. K. Gardner and L. Knopoff. Is the sequence of earthquakes in Southern California, with aftershocks removed, Poissonian? Bulletin of the Seismological Society of America 64 (5): 1363–1367. Oct. 1974. https://doi.org/10.1785/bssa0640051363.

[24] Motofumi Suzuki. A three dimensional box counting method for measuring fractal dimensions of 3D models. Proceedings of the 11th IASTED International Conference on Internet and Multimedia Systems and Applications, IMSA 2007. Jan. 2007.

[25] Paul Laurienti et al. Universal fractal scaling of self-organized networks. Nature Precedings 5. Sept. 2010. https://doi.org/10.1038/npre.2010.4894.1.

[26] Mavuto Mukaka. Statistics Corner: A guide to appropriate use of Correlation coefficient in medical research. Malawi medical journal: the journal of Medical Association of Malawi 24: 69–71. Sept. 2012.

[27] Mathieu Bastian, Sebastien Heymann, and Mathieu Jacomy. Gephi: An Open Source Software for Exploring and Manipulating Networks. 2009. http://www.aaai.org/ocs/index.php/ICWSM/09/paper/view/154.

[28] Feodor F. Dragan, Michel Habib, and Laurent Viennot. Revisiting Radius, Diameter, and all Eccentricity Computation in Graphs through Certificates. ArXiv abs/1803.04660. 2018.

[29] Vincent Blondel et al. Fast Unfolding of Communities in Large Networks. Journal of Statistical Mechanics Theory and Experiment 2008. Apr. 2008. https://doi.org/10.1088/1742-5468/2008/10/p10008.

[30] R. van der Hofstad. Configuration Model. Random Graphs and Complex Networks. Cambridge Series in Statistical and Probabilistic Mathematics. Cambridge University Press. 216–255. 2016. https://doi.org/10.1017/9781316779422.010.

[31] V. Traag, L. Waltman, and Nees Jan van Eck. From Louvain to Leiden: guaranteeing well-connected communities. Scientific Reports 9: 5233. Mar. 2019. https://doi.org/10.1038/s41598-019-41695-z.

[32] Nikolay Laptev et al. Time-series extreme event forecasting with neural networks at uber. International Conference on Machine Learning. 34. 1–5. 2017.

[33] Geophysics Department of the Aristotle University of Thessaloniki. http://geophysics.geo.auth.gr/ss/station_index_en.html (visited on June 1, 2020).

Appendix A Summary of results

Table A.1: Summary of results of this paper and related papers for each of the network models.

network model	this paper	related works
NTS(C)	• one component, no isolated nodes • when the seismic activity is high, the number of connections increases, which contributes to "shortcuts" emerging in the network • well-defined smaller local groups that constitute a network in time intervals with low seismicity are no longer clearly separated from each other when a large earthquake occurs • $\langle d \rangle$ and Q suddenly drop when a larger earthquake occurs • values of $\langle d \rangle$ and Q are smaller in networks consisting of larger cells	• scale-free and small-world • G-R law obtained • C and γ take the universal invariant values 0.85 and 1, respectively, when cell size becomes large than a certain threshold • C remains stationary before the large earthquake, suddenly jumps at the event, then slowly decays to stationarity again
MLN-NTSC(C)	• one component, no isolated nodes • when the seismic activity is high, the number of connections increases, which contributes to "shortcuts" emerging in the network • well-defined smaller local groups that constitute a network in time intervals with low seismicity are no longer clearly separated from each other when a large earthquake occurs • $\langle d \rangle$ and Q suddenly drop when a larger earthquake occurs • values of $\langle d \rangle$ and Q are smaller in networks consisting of larger cells • higher values of $\langle d \rangle$ and Q in networks consisting of multiple layers	• earthquake dynamics is better captured with a multilayer structure • nearby regions have similar seismic activity patterns
VG(E)	• each earthquake is always connected to its nearest neighbor in time • one component, no isolated nodes • hierarchical structure: weaker earthquakes that happened close together in time form groups that connect to each other through earthquakes of higher magnitudes, which results in the branching of a network • in time intervals with high seismicity, the branching is even more pronounced, as the hierarchical structure contributes to the long paths from one part of the network to the other • $\langle d \rangle$ and Q suddenly jump when a larger earthquake occurs	• scale-free • similar degree distributions for different threshold magnitudes • VG(E) structure depends only on the magnitude values • Omori law obtained
VG(C)	• one component, no isolated nodes • hierarchical structure observed in the VG(E) network is somewhat destroyed • when the seismic activity is high, the number of connections increases, which contributes to "shortcuts" emerging in the network • well-defined smaller local groups that constitute a network in time intervals with low seismicity are no longer clearly separated from each other when a large earthquake occurs • $\langle d \rangle$ and Q suddenly drop when a larger earthquake occurs • values of $\langle d \rangle$ and Q are smaller in networks consisting of larger cells	• G-R law obtained • Omori law obtained

SVG(E)	• because of the spatial component, earthquakes adjacent in time are no longer necessarily connected to each other (compared to the VG(E) network) • several components, quite a few isolated nodes • shape of the largest connected component is similar to the shape of the VG(E) network • in time intervals with high seismicity, some of the components connect with each other • $\langle d \rangle$ jumps and Q suddenly drops when a larger earthquake occurs	
SVG(C)	• several components, quite a few isolated nodes • in time intervals with high seismicity, some of the components connect with each other • hierarchical structure of the largest connected component observed in the SVG(E) network is somewhat destroyed • $\langle d \rangle$ jumps and Q suddenly drops when a larger earthquake occurs • when seismicity is low, the network consists of many small components that do not change much with the conversion from smaller to larger nodes • in time intervals with high seismicity, some differences can be observed when comparing networks composed of different cell sizes	
NTSW(E)	• several components, quite a few isolated nodes • the temporal and spatial windows of stronger earthquakes have a large temporal and spatial range • as a result, the network generated in the time intervals with high seismicity contains a higher number of connections than networks generated by other constructions	
NTSW(C)	• several components, quite a few isolated nodes • $\langle d \rangle$ jumps and Q suddenly drops when a larger earthquake occurs • when seismic activity is low, the network consists of many very small components that do not change much with the conversion from smaller to larger nodes • in time intervals with high seismicity, some differences can be observed when comparing networks composed of different cell sizes	• scale-free and small-world • G-R law obtained • Omori law obtained
NHTSW(E)	• several components, quite a few isolated nodes • the magnitude of an earthquake has a greater influence on the calculated value of n_{ij} compared to the product of time and distance • as a result, in the time intervals with high seismic activity, earthquakes lie very close in time and space • consequently, a very rough transition between the NHTSW(E) and NHTSW(C) constructions can be observed • $\langle d \rangle$ and Q suddenly drop when a larger earthquake occurs	• aftershocks identification • Omori law obtained • power law distribution of link weights and distances found
NHTSW(C)	• several components, quite a few isolated nodes • $\langle d \rangle$ and Q suddenly drop when a larger earthquake occurs	

NCV(C)	• cell vectors consist of almost only zero values, which means that the earthquakes in most of the cells occurred within the same time subinterval • possible connections in a network constitute mostly two types of pairs of vectors – those that contain a non-zero element at the same position of the vector ($r = 1$), and those that contain a non-zero element at different position of the vector, where all other elements in the vector are equal to 0 ($r = -1/(T-1)$) • several components in the form of well-defined groups • groups are the result of connections between cells with vectors composed of only one non-zero element • the non-zero element appears at the same position in all vectors in the same group • the number of groups in a network is equal to the number of elements in vectors belonging to the cells • cell vectors in one group differ from cell vectors in another group in the position of the non-zero element • in the time intervals with a stronger earthquake, depending on the time subinterval in which it occurs, some of the groups are more densely connected than others • cells corresponding to vectors with several non-zero elements can also be part of individual well-defined groups • as a result of connections between cells with vectors with multiple non-zero elements, shorter or longer paths can emerge in the network, starting in individual groups and connecting groups to each other • whether the network will contain such paths depends on the activity of the area, the distribution of earthquakes in the area, and the size of the cells • in time intervals with low seismicity, the value of modularity is close to 1 • the value of $\langle d \rangle$ and Q depends on the formation of shorter or longer paths that start in individual groups • as a result, the network produces time series with unreliable changes	• strong links found representing large correlations between patterns located more than 1000 km apart • networks of different periods are structurally similar